DISCLAIMER NOTICE

FOR REFERENCE ONLY AT EACH OF THE ASTIA OFFICES. THIS REPORT CANNOT BE SATISFACTORILY REPRODUCED; ASTIA DOES NOT FURNISH COPIES.

GD

GENERAL DYNAMICS
ASTRONAUTICS

351 760

A2136-1 (REV. 6-61)

ERR-AN-016
Aerophysics

ENVIRONMENTAL CONTROL STUDY

OF SPACE VEHICLES

(Part II)

Thermal Environment of Space

John C. Ballinger
Juan C. Elizalde
Rodolfo M. Garcia-Varela
Emmet H. Christensen

1 November 1960

Engineering Department

This work was supported under Convair sponsored research program number 111-9121

TABLE OF CONTENTS

FIGURES

TABLES

NOMENCLATURE

A = area, ft^2

a = albedo, non-dimensional

b = distance defined in Figure 8

d = radius defined in Figure 8

ds = element of planet surface area, ft^2

D = cylinder diameter, ft

F = view factor for flat plate, non-dimensional

L = length of cylinder, ft

h = altitude above planet surface, nautical miles

I_r = solar energy rate reflected per planet unit area, $Btu/hr\text{-}ft^2$

I_t = total energy rate emitted per planet unit area, $Btu/hr\text{-}ft^2$

I_α = energy rate emitted or reflected per planet unit area in the direction , $But/hr\text{-}ft^2$

q = radiant energy rate received by vehicle, Btu/hr

r = radius of sphere or hemisphere, ft

R = radius of the planet, nautical miles

S = solar constant, $Btu/hr\text{-}ft^2$

ρ = radius of integrating hemisphere, Figure 8

P = area of flat plate, ft^2

x = distance defined in Figure 8 or Figure 11

γ = angle between vertical to vehicle and cylinder or hemisphere axis or normal to flat plate, degrees

α = angle between normal to planetary element and vector to the vehicle, degrees

θ = spherical ordinate, degrees

θ_e = spherical ordinate of the horizon as seen from vehicle, degrees

ρ = distance between planet surface element and vehicle, nautical miles

ϕ = spherical abscissa, degrees

ϕ_c = angle of rotation of the axis of cylinder or hemisphere or normal to flat plate about a vertical to the vehicle, measured from the plane of the earth-vehicle and earth-sun vectors, degrees

Δ = angle between axis of cylinder or hemisphere or normal to flat plate and the vector from the vehicle to the planetary elemental area, degrees

δ = angle between vehicle-earth vector and the vector from the vehicle to the planetary elemental area, degrees

β = angle between earth-sun vector and extended normal to the planetary elemental area, degrees

ω = angle defined in Figure 8, degrees

ψ = angle defined in Figure 8, degrees

λ = angle defined in Figure 11, degrees

Subscripts

0, 1, 2, 3 etc. = refer to various intersections on the planetary sphere

ABSTRACT

A prerequisite to the [redacted] development of a system for the thermal control of a space vehicle is a clear and complete definition of the heat sources and sinks in space, and the modes and magnitudes of heat transfer. The study presented [redacted] is intended to provide this information, based upon the most reliable data [redacted] available. The curves and tabulated data given provide a complete mapping of the space thermal radiation environment throughout the solar system. Direct solar radiation, planetary albedo, and planetary thermal radiation are considered for vehicle surfaces of spherical, hemispherical, cylindrical and flat plate configurations. By combining these shapes and/or building up a composite of flat surfaces, heat incident to space vehicles of any configuration, located anywhere in the solar system can be obtained. For convenience, the bulk of the data is given in curve form in Supplement A* for hand computation and comparison purposes and in tabular form in Supplement B** for use as automatic digital computer data input.

In addition, internal heat loads, which are quite uncertain for future vehicles, are discussed in light of estimates based on presently proposed missions.

[redacted] work represents a portion of the study being performed under Convair Astronautics REA. 111-9121.

* AD-276 854

** AD-276 855

INTRODUCTION

Development or design of a system for controlling an environmental factor must have as a prerequisite a thorough understanding of the magnitude and character of that factor. In the case of thermal control for space vehicles it is necessary to clearly define the heat sources and sinks, and modes of heat transfer available in space. The study reported herein is intended to accomplish this, based on the most reliable information currently available. This represents the second part of a larger study program being conducted under Convair Astronautics REA 111-9121. The first part of the program was reported in References 1 and 2 and includes a detailed literature search of the subject and summaries of discussions held with a number of specialists in the field describing their current activities and proposed work. The following parts of this program will describe studies of control techniques and their effectiveness and application to the various phases of space flight and types of vehicles.

This report presents the results of parametric analyses of direct solar radiation, earth thermal radiation and albedo, to provide a means for defining vehicle external heat loads. Elemental vehicle shapes, including a plane surface, are considered with attitudes and altitudes as parameters. Use of the data presented, combining various shapes where necessary, will permit the calculation of the basic external heat load in space of any vehicle configuration. Internal heat loads, which are quite uncertain for future vehicles, are discussed in light of estimates based on presently proposed missions.

Environmental Analysis

The growing activity in the field of space vehicles has generated a similarly growing demand for means of maintaining safe operating temperatures within these vehicles. Removed from the atmosphere and its thermal influence, the space vehicle derives its temperature control through the regulation of thermal radiation. Temperature rise of an object in space must be the result of internal heat dissipation or radiation absorbed at its surface. Temperature fall must, in the long run, be the result of radiation emitted by the surface. Internal heat dissipation will in general, be defined by the specific mission requirements, leaving radiation control as the prime means of temperature regulation It is possible to use such schemes as evaporative mass transfer for cooling or internal electrical heaters for heating but such methods are not practical for long duration flights due to the payload penalty.

As a consequence, the study of temperature control for space vehicles must be focused on radiation control; which becomes meaningful only after a thorough knowledge of the thermal radiation environment in space has been obtained. This environment, for purposes of this report, will be referred to as Natural Thermal environment, in contrast to the term induced thermal environment which applies to the heat load generated by the vehicle operation, its crew and equipment. This natural thermal environment is made up essentially of three sources; direct solar radiation, planetary thermal radiation, and reflected solar radiation (planetary albedo). The contribution of each of these sources is analyzed in detail in the following sections. In addition, the much more nebulous problem of the induced thermal environment has been analyzed in a general manner. This type of treatment is the best that can be done until missions and vehicles become more firmly established and equipment details, which will continually change with the state of the art, become frozen for specific applications. This study, however, should provide a firm background for the evaluation of control techniques which is the next phase of the work to be covered under this REA. Further, it supplies all of the basic data necessary for a complete evaluation of the external heat load to which any space vehicle will be subjected and is readily usable for transient analyses where manual or digital computer techniques will be used.

A. Natural Thermal Environment

The origin of the thermal radiation environment in space is the sun. Direct solar radiation is obviously the most significant external heat source to a space vehicle, but depending upon the particular trajectory being flown, it may be followed closely by planetary thermal radiation and albedo. Planetary thermal radiation is basically the reradiation of solar energy previously absorbed by the planet surface or atmosphere. While planetary albedo, which is defined as diffuse reflectivity, is the fraction of total solar energy incident to the planet which is reflected away by its surface or atmosphere. It is clear, then, that the natural thermal environment for a vehicle traveling through space must be obtained by proper summing of these sources; and further that the variations in magnitude and direction of these heat loads, as seen by a vehicle, follow rather independent relationships. Consequently, the three sources are treated separately in the following sections, however, for albedo and thermal radiation, the same vehicle configurations are considered.

I. Solar Radiation

The sun radiates approximately as a black body with a surface temperature of about 10,000. degrees Fahrenheit. The thermal radiation received by an isolated body in space varies, for all practical purposes, inversely with the square of its distance to the sun. At earth's average distance (one astronomical unit) its mangitude, usually referred to as the solar constant, has been established as 442. $\pm 2\%$ $Btu/hr\text{-}ft^2$. This figure has been derived from the reduced data of a large number of measurements including rocket-borne spectrographs (Ref. 3, 4). Using this earth-distance value as a fiducial point, the variation of direct solar heat flux with distance to the sun, including appropriate values for the planets, is shown in Fig. 1. The solar heat fluxes for the planets are also listed in Table 1.

For the case of interplanetary flight, the space vehicle will be in direct sun light along practically all of its path. However, for an orbiting vehicle, in close proximity to a planet, the eclipsing or shadowing must be considered. The shadowed region in space is made up of the umbra or totally shaded area and the penumbra or partially shaded area in which a portion of the sun is still visible. An analysis of the influence, of passing through these regions, on the heat input to an actual vehicle clearly shows that the effect of the penumbra is quite small and may for most practical purposes be neglected. The umbra cone, however, can be very significant, resulting in a direct solar heat input reduction of greater than 40% for near orbits. Included in Table 1, are the umbra cone angles and apex altitudes for the various planets.

II. Planetary Thermal Radiation

Thermal energy is radiated by planets in the same manner as it is radiated by any heated body. The magnitude of this radiation depends on the surface temperature and its emission characteristics. The latter involves the properties of any atmosphere which may exist as well as the emissivity of the surface itself. Consequently, changes of atmospheric conditions, topography, season and time of day introduce variations in the planetary thermal radiation. However, neglecting details of the planet surface, it is possible to compute the average energy radiated by a planet using a thermal balance based on the solar radiation absorbed by the planet. As the temperatures of most planets do not vary appreciably over extended periods, it can be concluded that the thermally radiated energy is equivalent to the absorbed solar energy. Therefore, since the incident solar energy and average albedo are well known for most planets, the average thermal radiation can be readily calculated.

Using S as the solar heat flux per unit projected area of the planet (as seen from the sun), a as the planetary albedo, R as the planet radius, and I_t as the thermal energy radiated per average unit planet area and time, the energy balance is:

$$(1-a) S \pi R^2 = 4 \pi R^2 I_t \tag{1}$$

or

$$I_t = \left(\frac{1-a}{4}\right) S \tag{2}$$

Using the albedo values of Table 1, most of which was obtained from Ref. 5, and the solar heat flux data for the various planets from Fig. 1 or Table 1; the average planetary thermal radiations have been computed and are given also in Table 1.

Having thus established the magnitudes of the thermal radiation from the various planets, there remains only the calculation of this energy in space as it will be intercepted by a space vehicle. To make this analysis possible in a parametric manner, it is assumed that the planet

surface is radiating uniformly so that the average value applies to any region of the surface. In view of the velocities and types of trajectories which space craft may be expected to experience, this appears to be a reasonable assumption. In addition, since thermal radiation is only significant for altitudes less than about three planet diameters, the radiation is far from being parallel and consequently the vehicle external configuration must be specified for a heat flux value in space to be meaningful. The shapes considered in this study include the sphere, hemisphere, cylinder, and flat plate. In general any space vehicle shape could, for practical purposes, be analyzed as an assembly of flat plates, making it unnecessary to study, in parametric detail, specific configurations whose analytical treatments are appreciably more complex than that of the flat plate. Configurations other than those mentioned will, generally, be in this area of higher complexity.

For convenience of use only the thermal radiation heating data which has been calculated for the above configurations, is plotted in reference to the earth. To use these curves for a vehicle in the proximity of another planet it is only necessary to correct the altitude being considered to an equivalent earth altitude by multiplying it by the earth to new planet radius ration as given in Table 1, and using the appropriate planetary thermal radiation value (I_t) in the ordinate term.

a. Planetary Thermal Radiation to a Sphere

For a spherical body, the geometrical relationship shown in Fig. 2. The radiant heat flux, incident to a sphere of radius r, from the element of planet surface ds is

$$dq = \frac{\pi r^2 I_\alpha}{\rho^2} ds \tag{3}$$

where $I_\alpha = I_t \cos\alpha/\pi$ is the energy radiated in the direction determined by α .

Then:

$$dq = \frac{r^2 I_t \cos\alpha \, ds}{\rho^2} \tag{4}$$

Making the following substitutions:

$$H = h + R \tag{5}$$

$$\cos\alpha = \frac{H\cos\theta - R}{\rho} \tag{6}$$

$$ds = R^2 \sin\theta \, d\theta \, d\phi \tag{7}$$

$$\rho^2 = R^2 + H^2 - 2RH\cos\theta \tag{8}$$

The total incident heating rate from the planet to the sphere is.

$$q = 2r^2 R^2 I_t \int_0^{\pi}\int_0^{\theta_0} \frac{(H\cos\theta - R)\sin\theta}{(R^2 + H^2 - 2RH\cos\theta)^{3/2}}\, d\theta\, d\phi \qquad (9)$$

which after integration and substitution of $\cos\theta_0 = R/H$ yields.

$$q = 2\pi r^2 I_t \left(1 - \frac{\sqrt{2Rh + h^2}}{H}\right) \qquad (10)$$

Figure 3 shows the value $q/\pi r^2 I_t$ which is the planetary thermal radiation to a sphere per unit of great circle (or projected) area and per unit of surface thermal radiation, as a function of the altitude above the earth surface. The I_t term is included in the ordinate scale definition rather than in the curve plot itself to préclude obselescence of the curves in the event a more accurate value for earth albedo is determined in the future. At present there is a minor disagreement among the data of various investigators as to the exact value. The 0.40 value given in Table 1, appears to be the most likely value at present.

b. Planetary Thermal Radiation to a Cylinder

For a cylindrical body, the configuration is shown in Fig. 4. A new variable, the attitude of the cylinder with respect to the planet, defined by the angle γ, has to be considered.

The radiant heat flux incident to the lateral surface of a cylinder of diameter D and length L from the element of planet surface ds is:

$$dq = \frac{DL \sin\Delta \, I_t \cos\alpha \, ds}{\pi \rho^2} \tag{11}$$

where D L sin Δ is the projection of the cylinder surface as seen from ds, and $I_t \cos\alpha/\pi$ is the energy radiated in the direction α. The values of H, $\cos\alpha$, ds and ρ^2 are given again by equation (5) through (8)

The value of sin Δ is.

$$\sin\Delta = \sqrt{1 - (\cos\delta\cos\gamma + \sin\delta\sin\gamma\cos\phi)^2} \tag{12}$$

where

$$\cos\delta = \frac{H - R\cos\theta}{\rho} \tag{13}$$

$$\sin\delta = \frac{R\sin\theta}{\rho} \tag{14}$$

After substitutions and some algebraic manipulation, the total incident heat flux from the planet to the cylinder can be written as:

$$q = \frac{2DLI_tR^2}{\pi}\int_0^{\pi}\int_0^{\theta_0}\frac{(H\cos\theta - R)\sin\theta}{(H^2+R^2-2RH\cos\theta)^2} \times \sqrt{A + B\cos\phi - C\cos^2\phi}\; d\theta\, d\phi \tag{15}$$

where

$$A = R^2 + H^2 - H^2\cos^2\gamma - 2RH\cos\theta\sin^2\gamma - R^2\cos^2\theta\cos^2\gamma \tag{16}$$

$$B = 2R^2\sin\theta\cos\theta\sin\gamma\cos\gamma - 2RH\sin\theta\sin\gamma\cos\gamma \tag{17}$$

$$C = R^2\sin^2\theta\sin^2\gamma \tag{18}$$

The expression cannot be integrated analytically; a numerical integration is required. To perform this, and other numerical integrations mentioned later in the report, the solutions were programmed on an automatic digital computer. The results are plotted in Fig. 5, where the values of q/DLI_t are given as a function of the altitude above the earth surface h. with the attitude angle γ as a parameter.

To apply these curves to a vehicle in the proximity of a planet other than earth the same procedure and correction term as given for the case of the sphere and as listed in Table 1, may be used.

c. Planetary Thermal Radiation to a Hemisphere

For a hemispherical body, the configuration is shown in Fig. 6. The orientation parameter, γ for the hemisphere although similar to that for a cylinder, must assume values throughout 180° since the hemisphere is only symmetrical about one orthogonal axis.

The radiant heat flux incident to the hemispherical surface of radius r from the element of planet surface ds is:

$$dq = \frac{\tfrac{1}{2}\pi r^2(\cos\Delta+1)\, I_t \cos\alpha}{\pi \rho^2}\, ds \tag{19}$$

where $\tfrac{1}{2}\pi r^2(\cos\Delta+1)$ is the projection of the hemispherical surface as seen from ds and $I_t \cos\alpha/\pi$ is the energy radiated in the direction α. The values of H, $\cos\alpha$, ds and ρ^2 are given again by equations (5) through (8).

The value of $\cos\Delta$ is

$$\cos\Delta = \cos\delta\cos\gamma + \sin\delta\sin\gamma\cos\phi \tag{20}$$

where $\cos\delta$ and $\sin\delta$ are as defined in equations (13) and (14).

After substitutions and algebraic manipulation, the total incident heat flux from the planet to the hemispherical surface can be written as

$$q = I_t r^2 R^2 \left[\int_0^{\pi}\int_0^{\theta_0} \frac{(H\cos\theta - R)\sin\theta}{(H^2+R^2-2RH\cos\theta)^{3/2}}\, d\theta\, d\phi \right.$$
$$\left. + \int_0^{\pi}\int_0^{\theta_0} \frac{(H\cos\theta - R)\sin\theta\,(A + B\cos\phi)}{(H^2+R^2-2RH\cos\theta)^2}\, d\theta\, d\phi \right] \tag{21}$$

where

A = $H\cos\gamma - R\cos\theta\cos\gamma$

B = $R\sin\theta\sin\gamma$

The first term of the integration may be performed analytically to give the heat flux as follows,

$$q = I_t r^2 \left[\pi \left(1 - \frac{\sqrt{2Rh + h^2}}{H} \right) + R^2 \int_0^{\pi} \int_0^{\theta_0} \frac{(H\cos\theta - R)\sin\theta}{(H^2 + R^2 - 2RH\cos\theta)^2} (A + B\cos\phi)\, d\theta\, d\phi \right] \tag{22}$$

The second term was integrated numerically. The results are plotted in Fig. 7, where the gemetric factor $q/\pi r^2 I_t$ is given as a function of the altitude, h, above the earth's surface with the attitude angle γ as a parameter. These curves may be used for other planets as explained for the case of the sphere.

d. Planetary Thermal Radiation to a Flat Plate

For a flat plate a similar integration method may be used. However, a much similar solution can be found by resorting to a geometrical method of obtaining the view factor.

It can be proved that the view factor of a surface from a small flat plate can be geometrically determined as follows. The surface is projected from the viewing point onto a sphere having its center at the viewing point. The image on the sphere is then projected onto the plane of the small flat surface. The view factor is then determined from

$$F = \frac{\text{area projected on plane}}{\pi \rho^2}$$

where ρ is the radius of the sphere.

For our case the surface is the region of the planet which the flat plate can see, and the radius of the sphere is taken as the distance between the plate and the tangency point T, as shown in Fig. 8.

The general case is that in which the plane of the plate intersects the planet, and will be analyzed first.

The area of the circular segment A_1 is:

$$A_1 = \frac{\pi d^2 \omega_1}{360} - \frac{d^2 \sin \omega_1}{2} \tag{23}$$

To obtain the value of ω_1

$$\omega_1 = 180° - 2\psi \tag{24}$$

$$\psi = \sin^{-1} b/d \tag{25}$$

$$b = \frac{h + x}{\tan \delta} \tag{26}$$

$$h + x = p \sin\theta_0 \tag{27}$$

$$\sin\theta_0 = p/H \tag{28}$$

$$h + x = p^2/H \tag{29}$$

$$b = \frac{p^2}{H \tan\gamma} \tag{30}$$

$$d = p\cos\theta_0 = p\frac{R}{H} \tag{31}$$

$$\omega_1 = 180° - 2\sin^{-1}\frac{p}{R\tan\gamma} \tag{32}$$

and since $p = \sqrt{H^2 - R^2}$ (33)

$$\omega_1 = 180° - 2\sin^{-1}\frac{\sqrt{H^2 - R^2}}{R\tan\gamma} \tag{34}$$

The area A_1 is substracted from πd^2 to give A_2

The area of the circular segment A_3 is:

$$A_3 = \frac{\pi p^2 \omega_2}{360} - \frac{p^2 \sin\omega_2}{2} \tag{35}$$

For a similar way as for ω_1 it can be found that:

$$\omega_2 = 180^\circ - 2\sin^{-1}\frac{\sqrt{H^2-R^2}}{H\sin\gamma} \tag{36}$$

Then, projecting the areas A_2 and A_3 on the plane of the flat plate, and dividing the sum of their projections by $\pi\rho^2$ the view factor is obtained.

The resulting expression is:

$$\begin{aligned} F = \frac{1}{360}&\left[180^\circ - 2\sin^{-1}\frac{\sqrt{H^2-R^2}}{H\sin\gamma}\right] \\ &- \frac{1}{2\pi}\sin\left[2\sin^{-1}\left(\frac{\sqrt{H^2-R^2}}{H\sin\gamma}\right)\right] + \left\{\frac{R^2}{H^2}\right. \\ &- \frac{1}{360}\frac{R^2}{H^2}\left[180^\circ - 2\sin^{-1}\left(\frac{\sqrt{H^2-R^2}}{R\tan\gamma}\right)\right] \\ &\left.+ \frac{1}{2\pi}\frac{R^2}{H^2}\sin\left[2\sin^{-1}\left(\frac{\sqrt{H^2-R^2}}{R\tan\gamma}\right)\right]\right\}\cos\gamma \end{aligned} \tag{37}$$

A much simpler expression is obtained when the plane of the plate does not intersect the planet. In that case, $A_1 = A_3 = 0$ and $A_2 = \pi d^2$

Then:

$$F = \frac{A_2\cos\gamma}{\pi\rho^2} = \frac{R^2}{H^2}\cos\gamma \tag{38}$$

In either case, the total heat flux from the planet to the flat plate is given by:

$$q = I_t F P \tag{39}$$

where P is the area of the plate. Figure 9, shows a plotting of the thermal radiation to a flat place as a function of altitude with the attitude angle γ as a parameter. Again, to apply these curves to planets other than the earth, the procedure given for the sphere may be used.

III. Planetary Albedo

As mentioned earlier in the report, planetary albedo is the ratio of reflected to total incident solar radiation. As such, the units of the term albedo are unity, however, as the expression has been being brought into discussions more and more frequently in recent years it is now often being used to mean the reflected energy itself. Whatever the final precise definition of the term, it clearly differentiates the portion of the incident solar energy which is reflected by the planet from that which is absorbed and reradiated.

The average albedo for planets located up to 10 astronomical units from the sun is known with reasonable accuracy, the value for the earth being the least accurate. Extreme values of .29 to .52 for the earth are considered acceptable for specific times due to daily as well as seasonal variations in cloudiness and surface conditions. The value of 0.40 has been selected as a likely average and is given in Table 1. This value, which has been frequently used in the past may be superseded in the future by a number closer to .36 which has been recommended by Dr. Sigmund Fritz who has compiled a number of recent measurements made in diverse areas of the world under varying weather conditions. The current satellite programs will undoubtly provide a highly refined evaluation of this in the future.

At distances greater than about 10 astronomical units from the sun the accuracy of the planetary albedo falls off significantly, due to the very small magnitude of the reflected energy.

To permit a parametric analysis of the solar energy reflected from a planet, the same assumption which was made for thermal radiation; viz. a uniform planet surface with regard to radiation characteristics, will be made. It is further assumed that the planet surface reflects diffusely i.e., it obeys Lambert's Law. While these assumptions may not be entirely accurate, particularly for the earth where large bodies of water exist;

their use can in general be fully justified by consideration of trajectories, orbits and velocities which the vehicles, that are being used in the analysis, will experience.

Based upon these assumptions it is clear that the reflected energy will have a cosine distribution, not only with respect to the angular radiation from a given area, but over the sunlit surface of the planet as well. This considerably complicates the problem over the case of thermal radiation with the result that a direct analytical solution is not available even for the case of a spherical vehicle, and for the cases of vehicles other than a sphere the number of computations is greatly increased due to the increased number of variables. The result is that some 97 pages of curves are necessary to adequately describe reflected heating to the sphere, hemisphere, cylinder and flat plate which were used in the thermal radiation analyses. As a consequence of the bulk involved, these albedo heating data curves are being published as Supplement "A" to this report, while the same data, in tabular form, especially useful as computer program input tables are being published as Supplement "B".

As in the case of the thermal radiation analysis, the heating data is plotted in reference to the earth. Also, the data may be used for vehicles in the proximity of other planets by applying the same radius ratio correction terms to obtain an equivalent earth altitude, and then using the appropriate ordinate multiplying factor given in Table 1. This factor takes into account the albedo and solar heat input to the planet considered.

a. Albedo Radiation to a Sphere

Considering the reflected (or albedo) heat flux incident to a sphere in space, the most general configuration is given in Fig. 10. As in the case of thermal radiation, this heat flux to a sphere of radius r from the element of planet surface ds, is:

$$dq = \frac{\pi r^2 I_\alpha \, ds}{\rho^2} \tag{40}$$

where $I_\alpha = I_r \cos\alpha / \pi$ is the fraction of reflected solar radiation in the direction determined by α. It is the total reflected energy per unit of planet surface, and is given by:

$$I_r = Sa \cos\beta \tag{41}$$

Where S is the direct solar heat flux normal to the sun direction, a, the albedo and β, the angle between the vertical to the planet surface at ds and the direction to the sun, as shown in Fig. 10. Then,

$$dq = \frac{r^2}{\rho^2} S a \cos\alpha \cos\beta \, ds \tag{42}$$

$\cos\alpha$, ds and ρ^2 are given by (6), (7), and (8).

The value of $\cos\beta$ is:

$$\cos\beta = \cos\theta\cos\theta_s + \sin\theta\sin\theta_s\cos\phi \tag{43}$$

where θ_s is the angle between the heated body and the sun.

Substituting these expressions in (42) and integrating for θ and ϕ, q can be obtained. However, careful consideration has to be given to the limits of integration. Two cases should be considered, as illustrated in Fig. 11. The first one occurs when the region of the planet seen from the satellite is completely sunlit. This condition can be expressed as ($\theta_0 \leq \pi/2 - \theta_s$), and the limits of integration are 0 and θ_0 for θ, 0 and π for ϕ (the integral with respect to ϕ is multiplied by 2). When the region of the planet seen from the satellite is only partially sunlit ($\theta_0 > \pi/2 - \theta_s$), a variable upper limit for ϕ has to be introduced. It is convenient to perform the integration for two regions: the first region (labeled 1 in the figure) is totally sunlit, and the limits are 0 to $\pi/2 - \theta_s$ for θ, 0 to π for ϕ. The limits for region 2 are $\pi/2 - \theta_s$ to θ_0 for θ and 0 to $\pi/2 + \sin^{-1}(\operatorname{ctg}\theta_s \operatorname{ctg}\theta)$ for ϕ. This variable limit can be obtained as follows. From Fig. 11, it is immediate that

$$\phi = \pi/2 + \lambda \tag{44}$$

Also $$x = R\cos\theta \,\mathrm{ctg}\,\theta_s \tag{45}$$

and $$\sin\lambda = \frac{x}{R\sin\theta} = \mathrm{ctg}\,\theta_s \,\mathrm{ctg}\,\theta \tag{46}$$

Therefore $$\phi = \pi/2 + \sin^{-1}(\mathrm{ctg}\,\theta_s \,\mathrm{ctg}\,\theta) \tag{47}$$

Finally by adding the integrals over regions 1 and 2, the total solar radiation reflected by the planet incident upon the sphere is:

$$q = 2r^2 S a R^2 \left[\int_0^{\pi/2-\theta_s} \int_0^{\pi} \frac{(H\cos\theta - R)(\cos\theta\cos\theta_s + \sin\theta\sin\theta_s\cos\phi)\sin\theta\, d\theta\, d\phi}{(R^2+H^2-2RH\cos\theta)^{3/2}} \right.$$
$$\left. + \int_{\pi/2-\theta_s}^{\theta_0} \int_0^{\pi/2+\sin^{-1}(\mathrm{ctg}\,\theta_s \,\mathrm{ctg}\,\theta)} \frac{(H\cos\theta - R)(\cos\theta\cos\theta_s + \sin\theta\sin\theta_s\cos\phi)\sin\theta\, d\theta\, d\phi}{(R^2+H^2-2RH\cos\theta)^{3/2}} \right] \tag{48}$$

This equation holds for $\theta_s < \pi/2$. For $\theta_s \geq \pi/2$ the first term of (48) disappears and the lower lower limit on θ of the second term becomes $\theta_s - \pi/2$

Integration with respect to ϕ is immediate, not so with respect to θ which requires a numerical method. Figure 12 shows the value of $q/\pi r^2 S a$ which is the heat flux to a sphere per unit of great circle (projected) area per unit of reflected solar radiation; as a function of altitude above the earth surface, with θ_s as a parameter.

b. Albedo to a Cylinder

Like the solution for albedo to a sphere, the albedo to a cylinder is computed by a similar numerical method, however the integrand is more complex since two additional parameters defining the attitude of the cylinder must be included. The general configuration is shown in Fig. 13.

The radiant heat flux incident to the cylinder lateral surface of diameter D and length L due to reflected solar energy from the element of planet surface ds is:

$$dq = \frac{D L I_\alpha \sin\Delta \, ds}{\rho^2} \tag{49}$$

where $I_\alpha = I_r \cos\alpha / \pi$ is the fraction of reflected solar radiation in the direction determined by α . I_r is the total reflected energy per unit of planet surface, and is given by equation (41) where S is the direct solar heat flux normal to the sun direction, a is the albedo and β is the angle between the normal to the planet surface and ds and the direction to the sun as shown in Fig. 13.

$DL \sin\Delta$ is the projection of the lateral surface of the cylinder as seen from ds. With the symbols defined, the elemental incident flux to the cylinder may be written

$$dq = \frac{D L S a \cos\beta \cos\alpha \sin\Delta \, ds}{\pi \rho^2} \tag{50}$$

$\cos\alpha$, ds, and ρ^2 are given by (6), (7), and (8)

$\sin\Delta$ is given by

$$\sin\Delta = \left\{1 - \left[\cos\delta \cos\gamma + \sin\delta \sin\gamma \cos(\phi - \phi_c)\right]^2\right\}^{1/2} \tag{51}$$

where $\cos\delta$ and $\sin\delta$ are as defined in equations (13) and (14). The angle ϕ_c is one of the attitude parameters being the angle of rotation of the cylinder axis about a vertical to the cylinder. $\phi_c = 0$ when the axis lies in the plane containing the earth-cylinder vector and the earth-sun vector. The angle γ is the other attitude parameter being the angle between the vertical to the cylinder and the axis of the cylinder.

The value of $\cos\beta$ may be expressed as given in (43), where θ_s is as defined for albedo to a sphere and may be referred to as the zenith distance from the vehicle to the sun and θ and ϕ are the variables of integration. After substitution and integrating with respect to θ and ϕ, q can be obtained. Again as in the case of a sphere two cases should be considered, the first being when the entire area of the planet seen from the cylinder is sunlit, and the second being when the area is only partially sunlit, i.e., the satellite can see a portion of the terminator, in which case a variable limit for ϕ is required and is again given by (47). Recognizing symmetry about the plane containing the earth-vehicle vector and the earth sun vector total reflected solar heat flux from the planet incident on the cylindrical surface can be written for $\theta_s < \pi/2$ as:

$$q = \frac{2DLSaR^2}{\pi}\left[\int_0^{\pi/2-\theta_s}\int_0^{\pi}\frac{A\cdot B\cdot C\cdot D}{E^2}\,d\theta\,d\phi + \int_{\pi/2-\theta_s}^{\theta_s}\int_0^{\pi/2+\sin^{-1}(\operatorname{ctg}\theta_s\operatorname{ctg}\theta)}\frac{A\cdot B\cdot C\cdot D}{E^2}\,d\theta\,d\phi\right] \tag{52}$$

where
$$A = H\cos\theta - R$$
$$B = \cos\theta_s\cos\theta + \sin\theta_s\sin\theta\cos\phi$$
$$C = \sin\theta$$
$$D = \sqrt{R^2+H^2-2RH\sin^2\gamma\cos\theta - H^2\cos^2\gamma - R^2\cos^2\gamma\cos\theta - 2RH\cos\gamma\sin\gamma\sin\theta\cos(\phi-\phi_c) + 2R^2\cos\gamma\sin\gamma\sin\theta\cos\theta\cos(\phi-\phi_c) - R^2\sin^2\gamma\sin^2\theta\cos^2(\phi-\phi_c)}$$
$$E = R^2 + H^2 - 2RH\cos\theta$$

When $\pi/2 \leq \theta_s \leq \pi/2 + \theta_0$ the integration limits change and integration occurs over only one zone with limits given as follows

$$q = \frac{2DLSaR^2}{\pi} \int_{\theta_0 - \pi/2}^{\theta_0} \int_0^{\pi/2 + \sin^{-1}(ctg\,\theta_s\, ctg\,\theta)} \frac{A \cdot B \cdot C \cdot D}{E^2}\, d\theta\, d\phi \tag{53}$$

The heat flux integrals (52) and (53) have been integrated numerically on an IBM 704 computer. The results are displayed as the geometric factor, $(q/DLSa)$ as a function of altitude with zenith distance, θ_s, angle between the vertical to the cylinder and the cylinder axis γ and angle of rotation, ϕ_c, of the axis of the cylinder about the vertical to the cylinder referenced to the plane containing the vertical and the earth-sun vector as the three parameters. This graphical presentation required 22 sheets, each for a constant γ and ϕ_c and are presented in Supplement A. The values considered for the attitude parameters were γ = 0°, 30°, 60°, and 90° and simultaneously ϕ_c = 0°, 30°, 60°, 90°, 120°, 150°, and 180°. The parameter γ need only be considered to 90° as the cylinder has end-for-end symmetry.

The geometric factors computed for the earth may be applied to other planets by applying the radius ratio correction term and ordinate multiplying factor of Table 1, as described for albedo to a a sphere.

c. Albedo to a Hemisphere

The solution for albedo to a hemisphere is very similar to that for a cylinder, the two major differences being that the expression for the projected area of the hemisphere with respect to ds is somewhat different and that values of γ from 0 to 180° must be considered as end-for-end symmetry is not present. The general configuration for albedo to a hemisphere is shown in Fig. 14.

The radiant heat flux incident to the hemispherical surface of radius, r, due to reflected solar energy from the planet surface, ds is:

$$dq = \frac{1/2\,\pi r^2 (1+\cos\Delta)\, I_\alpha\, ds}{\rho^2} \tag{54}$$

where $1/2\,\pi r^2 (1+\cos\Delta)$ is the projected area of the hemispherical surface as seen from ds and the remaining symbols are as defined for a cylinder. Recognizing the symbols of (54) to be defined the same as for a cylinder, the elemental incident heat flux to a hemisphere may be written

$$dq = \frac{1/2\,\pi r^2\, Sa \cos\beta \cos\alpha\, (1+\cos\Delta)\, ds}{\pi \rho^2} \tag{55}$$

$\cos\Delta$ is given by

$$\cos\Delta = \cos\gamma\cos\delta + \sin\gamma\sin\delta\cos(\phi-\phi_c) \tag{56}$$

with the terms defined as for the cylinder solution.

$\cos\beta$ is again given by equation (43)

$\cos\alpha$, ds and ρ^2 are given by (6), (7), and (8).

The integration techniques and limits are as defined for albedo to a cylinder. The total reflected solar heat flux from the planet incident on the hemispherical surface can be written for $\theta_s < \pi/2$ as

$$q = r^2 S a R^2 \left[\int_0^{\pi/2-\theta_s} \int_0^{\pi} \frac{A \cdot B \cdot C \cdot (\sqrt{E} + F)}{E^2} \, d\theta \, d\phi \right.$$

$$\left. + \int_{\pi/2-\theta_s}^{\theta_0} \int_0^{\pi/2+\sin^{-1}(ctg\,\theta_s\, ctg\,\theta)} \frac{A \cdot B \cdot C\,(\sqrt{E} + F)}{E^2} \, d\theta \, d\phi \right] \tag{57}$$

where

A = $H\cos\theta - R$
B = $\cos\theta_s \cos\theta + \sin\theta_s \sin\theta \cos\phi$
C = $\sin\theta$
E = $R^2 + H^2 - 2RH\cos\theta$
F = $H\cos\gamma - R\cos\gamma\cos\theta + R\sin\gamma\sin\theta\cos(\phi - \phi_c)$

When $\pi/2 \leq \theta_s \leq \pi/2 + \theta_0$ the heat flux to the hemisphere is

$$q = r^2 S a R^2 \int_{\theta_s-\pi/2}^{\theta_0} \int_0^{\pi/2+\sin^{-1}(ctg\,\theta_s\, ctg\,\theta)} \frac{A \cdot B \cdot C\,(\sqrt{E} + F)}{E^2} \, d\theta \, d\phi \tag{58}$$

The heat flux integrals (57) and (58) have been integrated numerically on an IBM 7090 computer. The results are displayed as the geometric factor $q/\pi r^2 S a$ as a function of altitude with the three angles θ_s, γ and ϕ_c as parameters. This graphical presentation required 37 sheets, each for a constant γ and ϕ_c and are presented in supplement A.

The values considered for the attitude parameters were $\gamma = 0°, 30°, 60°, 90°, 120°, 150°,$ and $180°$ and simultaneously $\phi_c = 0°, 30°, 60°, 90°, 120°, 150°,$ and $180°$.

Again the geometric factors computed for the earth may be applied to other planets by applying the radius ratio correction term and ordinate multiplying factor of Table 1, as described for albedo to a sphere.

d. Albedo to a Flat Plate

Considering the albedo heat flux incident on one side of a flat plate in space, the most general configuration is given in Fig. 15. Development of the integral takes the same form as that for a cylinder or a hemisphere. The heat flux incident to a flat plate of area, P, from the element of planet surface, ds, is:

$$dq = \frac{P \cos \Delta \, I_\alpha \, ds}{\rho^2} \tag{59}$$

where $P \cos \Delta$ is the projected area of the plate as seen from ds. Recognizing the remaining symbols to be defined as for a cylinder (59) may be written as

$$dq = \frac{P S a \cos \beta \cos \alpha \cos \Delta \, ds}{\pi \rho^2} \tag{60}$$

$\cos \gamma$, ds and ρ^2 are given by (6), (7), and (8).

$\cos \beta$ is again given by equation (43).

$\cos \Delta$ is given by equation (56) with the terms defined as for the cylinder solution. The total reflected solar heat flux from the planet incident on the flat plate can be written as an indefinite integral.

$$q = \frac{PSaR^2}{\pi} \int_{\theta}\int_{\phi} \frac{A \cdot B \cdot C \cdot (G+F)}{E^2}\, d\theta\, d\phi \tag{61}$$

where A, B, C and E are as defined for a cylinder

F = $R \sin\gamma \sin\theta \cos(\phi - \phi_c)$

G = $\cos\gamma (H - R\cos\theta)$

The problem of limits for the integration of (61) is severely complicated by the fact that the plane of the flat plate may cut off portions of the sunlit area of the planet.

The limits considered are discussed with respect to the computer solution of equation (61). Two major conditions are considered, one is if the flat plate sees the sunlit surface of the planet with the plane in which it lies not cutting any portion of the sunlet area, the other is if the plane of the flat plate cuts the sunlit area. If the plane does not cut the sunlit area, two conditions may be involved. Either the plane sees a full sunlit zone, i.e., does not see the terminator, in which case equation (61) becomes

$$q = \frac{2PSaR^2}{\pi} \int_{0}^{\theta_0}\int_{0}^{\pi} \frac{A \cdot B \cdot C \cdot (G+F)}{E^2}\, d\theta\, d\phi \tag{62}$$

or the plane sees part of the terminator in which case when $\theta_s < \pi/2$ (62) becomes

$$q = \frac{2PSaR^2}{\pi}\left[\int_0^{\pi/2-\theta_s}\int_0^{\pi}\frac{A\cdot B\cdot C\cdot(G+F)}{E^2}\,d\theta\, d\phi\right.$$

$$\left.+\int_{\pi/2-\theta_s}^{\theta_0}\int_0^{\pi/2+\sin^{-1}(ctg\,\theta_s\, ctg\,\theta)}\frac{A\cdot B\cdot C\,(G+F)}{E^2}\,d\theta\, d\phi\right] \tag{63}$$

when $\pi/2 \leq \theta_s \leq \pi/2+\theta_0$

$$q = \frac{2PSaR^2}{\pi}\left[\int_{\theta_s-\pi/2}^{\theta_0}\int_0^{\pi/2+\sin^{-1}(ctg\,\theta_s\, ctg\,\theta)}\frac{A\cdot B\cdot C\cdot(G+F)}{E^2}\,d\theta\, d\phi\right] \tag{64}$$

The problem becomes more complex when the plane cuts the sunlit area as the limits of θ and ϕ are determined by more complex equations. If the plane cuts the sunlit area but the plane does not see the terminator, equation (61) becomes for $\theta_s < \pi/2$ and $\gamma < \pi/2$,

$$q = \frac{PSaR^2}{\pi}\left[\int_0^{\theta_1}\int_{-\pi}^{\pi}\frac{A\cdot B\cdot C\cdot(G+F)}{E^2}\,d\theta\,d\phi\right.$$

$$\left.+\int_{\theta_1}^{\theta_0}\int_{-\left[\frac{\pi}{2}-\phi_c+\sin^{-1}\left\{\frac{\tan\left[\cos^{-1}\left(\frac{R\sin\theta}{\sqrt{R^2+H^2-2RH\cos\theta}}\right)\right]}{\tan\gamma}\right\}\right]}^{\frac{\pi}{2}+\phi_c+\sin^{-1}\left\{\frac{\tan\left[\cos^{-1}\left(\frac{R\sin\theta}{\sqrt{R^2+H^2-2RH\cos\theta}}\right)\right]}{\tan\gamma}\right\}}\frac{A\cdot B\cdot C\cdot(G+F)}{E^2}\,d\theta\,d\phi\right] \tag{65}$$

where θ_1 was determined from the equation

$$\pi/2 = \sin^{-1}\left\{\frac{\tan\left[\cos^{-1}\left(\frac{R\sin\theta_1}{\sqrt{R^2+H^2-2RH\cos\theta_1}}\right)\right]}{\tan\gamma}\right\} \tag{66}$$

by the Newton-Raphson iteration procedure for determining roots. For $\pi/2 < \gamma < \pi/2 + \theta_0$, q is given by equation (65) with the first integral term eliminated. It should be noted that for $\gamma > \pi/2 + \theta_0$, $q = 0$, i.e., the plane surface does not see the earth.

A number of forms of the equation (61) are possible if the plane of the flat plate cuts the sunlit area and also sees a portion of the terminator. For the case where the plane of the flat plate for $\gamma < \pi/2$ intersects the terminator in two points (ϕ_3, θ_3) and (ϕ_4, θ_4) and θ_3 and $\theta_4 > \theta_0$, $\phi_3 > \phi_4$, $\phi_4 < \pi$ equation (61) becomes

$$q = \frac{PSaR^2}{\pi}\left[\int_0^{\theta_1}\int_{-\pi}^{\pi}\frac{A\cdot B\cdot C\cdot(G+F)}{E^2}\,d\theta\,d\phi\right.$$

$$+\int_{\theta_1}^{\theta_4}\int_{-\left[\pi/2-\phi_c+\sin^{-1}\left\{\frac{\tan\left[\cos^{-1}\left(\frac{R\sin\theta}{\sqrt{R^2+H^2-2RH\cos\theta}}\right)\right]}{\tan\gamma}\right\}\right]}^{\pi/2+\phi_c+\sin^{-1}\left\{\frac{\tan\left[\cos^{-1}\left(\frac{R\sin\theta}{\sqrt{R^2+H^2-2RH\cos\theta}}\right)\right]}{\tan\gamma}\right\}}\frac{A\cdot B\cdot C(G+F)}{E^2}\,d\theta\,d\phi$$

$$+\int_{\theta_4}^{\theta_3}\int_{-\left[\frac{\pi}{2}-\phi_c+\sin^{-1}\left\{\frac{\tan\left[\cos^{-1}\left(\frac{R\sin\theta}{\sqrt{R^2+H^2-2RH\cos\theta}}\right)\right]}{\tan\gamma}\right\}\right]}^{\pi/2+\sin^{-1}(\mathrm{ctg}\,\theta_5\,\mathrm{ctg}\,\theta)}\frac{A\cdot B\cdot C\cdot(G+F)}{E^2}\,d\theta\,d\phi$$

$$\left.+\int_{\theta_3}^{\theta_5}\int_{-\left[\pi/2+\sin^{-1}(\mathrm{ctg}\,\theta_5\,\mathrm{ctg}\,\theta)\right]}^{\pi/2+\sin^{-1}(\mathrm{ctg}\,\theta_5\,\mathrm{ctg}\,\theta)}\frac{A\cdot B\cdot C(G+F)}{E^2}\,d\theta\,d\phi\right]; \tag{67}$$

where θ_4 & θ_3 were determined by the Newton-Raphson method from the following equations, respectively.

$$\sin^{-1}(\mathrm{ctg}\,\theta_5\,\mathrm{ctg}\,\theta_4) = \phi_c + \sin^{-1}\left\{\frac{\tan\left[\cos^{-1}\left(\frac{R\sin\theta_4}{\sqrt{R^2+H^2-2RH\cos\theta_4}}\right)\right]}{\tan\gamma}\right\} \tag{68}$$

and

$$-\sin^{-1}(\text{ctg}\,\theta_s\,\text{ctg}\,\theta_3) = \phi_c - \sin^{-1}\left\{\frac{\tan\left[\cos^{-1}\left(\frac{R\sin\theta_3}{\sqrt{R^2+H^2-2RH\cos\theta_3}}\right)\right]}{\tan\gamma}\right\} \quad (69)$$

For $\phi_4 > \pi$ two conditions may be considered. If $\pi/2 - \theta_s < \theta_1$ equation (61) becomes

$$\begin{aligned}
q = \frac{PSaR^2}{\pi}\Bigg[& \int_0^{\pi/2-\theta_s}\int_{-\pi}^{\pi}\frac{A\cdot B\cdot C(G+F)}{E^2}\,d\theta\,d\phi \\
& + \int_{\pi/2-\theta_s}^{\theta_1}\int_{-[\pi/2+\sin^{-1}(\text{ctg}\,\theta_s\,\text{ctg}\,\theta)]}^{\pi/2+\sin^{-1}(\text{ctg}\,\theta_s\,\text{ctg}\,\theta)}\frac{A\cdot B\cdot C\cdot(G+F)}{E^2}\,d\theta\,d\phi \\
& + \int_{\theta_1}^{\theta_4}\int_{-[\pi/2+\sin^{-1}(\text{ctg}\,\theta_s\,\text{ctg}\,\theta)]}^{\pi/2+\phi_c+\sin^{-1}\left\{\frac{\tan\left[\cos^{-1}\left(\frac{R\sin\theta}{\sqrt{R^2+H^2-2RH\cos\theta}}\right)\right]}{\tan\gamma}\right\}}\frac{A\cdot B\cdot C(G+F)}{E^2}\,d\theta\,d\phi \\
& + \int_{\theta_1}^{\theta_3}\int_{-\left[\pi/2-\phi_c+\sin^{-1}\left\{\frac{\tan\left[\cos^{-1}\left(\frac{R\sin\theta}{\sqrt{R^2+H^2-2RH\cos\theta}}\right)\right]}{\tan\gamma}\right\}\right]}^{\pi/2+\sin^{-1}(\text{ctg}\,\theta_s\,\text{ctg}\,\theta)}\frac{A\cdot B\cdot C(G+F)}{E^2}\,d\theta\,d\phi \\
& + \int_{\theta_3}^{\theta_0}\int_{-[\pi/2+\sin^{-1}(\text{ctg}\,\theta_s\,\text{ctg}\,\theta)]}^{\pi/2+\sin^{-1}(\text{ctg}\,\theta_s\,\text{ctg}\,\theta)}\frac{A\cdot B\cdot C(G+F)}{E^2}\,d\theta\,d\phi\Bigg]
\end{aligned} \quad (70)$$

θ_3 is determined by equation (69)

θ_4 is determined by the following equation

$$\pi + \sin^{-1}(\operatorname{ctg}\theta_s \operatorname{ctg}\theta_4) = \phi_c + \sin^{-1}\left\{\frac{\tan\left[\cos^{-1}\left(\frac{R\sin\theta_4}{\sqrt{R^2+H^2-2RH\cos\theta_4}}\right)\right]}{\tan\gamma}\right\} \tag{71}$$

If $\pi/2 - \theta_s > \theta_1$ the limits change somewhat.

$$q = \frac{PSaR^2}{\pi}\left[\int_0^{\theta_1}\int_{-\pi}^{\pi}\frac{A\cdot B\cdot C\cdot(G+F)}{E^2}\,d\theta\,d\phi\right.$$

$$+\int_{\theta_1}^{\pi/2-\theta_s}\int_{-\left[\pi/2-\phi_c+\sin^{-1}\left\{\frac{\tan\left[\cos^{-1}\left(\frac{R\sin\theta}{\sqrt{R^2+H^2-2RH\cos\theta}}\right)\right]}{\tan\gamma}\right\}\right]}^{\pi/2+\phi_c+\sin^{-1}\left\{\frac{\tan\left[\cos^{-1}\left(\frac{R\sin\theta}{\sqrt{R^2+H^2-2RH\cos\theta}}\right)\right]}{\tan\gamma}\right\}}\frac{A\cdot B\cdot C\cdot(G+F)}{E^2}\,d\theta\,d\phi$$

$$+\int_{\pi/2-\theta_s}^{\theta_4}\int_{-\left[\pi/2+\sin^{-1}(\operatorname{ctg}\theta_s\operatorname{ctg}\theta)\right]}^{\pi/2+\phi_c+\sin^{-1}\left\{\frac{\tan\left[\cos^{-1}\left(\frac{R\sin\theta}{\sqrt{R^2+H^2-2RH\cos\theta}}\right)\right]}{\tan\gamma}\right\}}\frac{A\cdot B\cdot C\cdot(G+F)}{E^2}\,d\theta\,d\phi$$

$$+\int_{\pi/2-\theta_s}^{\theta_3}\int_{-\left[\pi/2-\phi_c+\sin^{-1}\left\{\frac{\tan\left[\cos^{-1}\left(\frac{R\sin\theta}{\sqrt{R^2+H^2-2RH\cos\theta}}\right)\right]}{\tan\gamma}\right\}\right]}^{\pi/2+\sin^{-1}(\operatorname{ctg}\theta_s\operatorname{ctg}\theta)}\frac{A\cdot B\cdot C\,(G+F)}{E^2}\,d\theta\,d\phi$$

$$\left.+\int_{\theta_3}^{\theta_0}\int_{-\left[\pi/2+\sin^{-1}(\operatorname{ctg}\theta_s\operatorname{ctg}\theta)\right)}^{\pi/2+\sin^{-1}(\operatorname{ctg}\theta_s\operatorname{ctg}\theta)}\frac{A\cdot B\cdot C\,(G+F)}{E^2}\,d\theta\,d\phi\right] \tag{72}$$

For the case where the plane of the flat plate intersects the terminator in one point (ϕ_4, θ_4) and the circle defined by $\theta = \theta_0$ in one point (ϕ_3, θ_0) and $\phi_4 < \pi$ equation (61) becomes

$$q = \frac{PSaR^2}{\pi}\left[\int_0^{\theta_1}\int_{-\pi}^{\pi} \frac{A\cdot B\cdot C\cdot(G+F)}{E^2}\,d\theta\,d\phi \right.$$

$$+\int_{\theta_1}^{\theta_4}\int_{-\left[\pi/2-\phi_c+\sin^{-1}\left\{\frac{\tan\left[\cos^{-1}\left(\frac{R\sin\theta}{\sqrt{R^2+H^2-2RH\cos\theta}}\right)\right]}{\tan\gamma}\right\}\right]}^{\pi/2+\phi_c+\sin^{-1}\left\{\frac{\tan\left[\cos^{-1}\left(\frac{R\sin\theta}{\sqrt{R^2+H^2-2RH\cos\theta}}\right)\right]}{\tan\gamma}\right\}} \frac{A\cdot B\cdot C\cdot(G+F)}{E^2}\,d\theta\,d\phi$$

$$\left.+\int_{\theta_4}^{\theta_0}\int_{-\left[\pi/2-\phi_c+\sin^{-1}\left\{\frac{\tan\left[\cos^{-1}\left(\frac{R\sin\theta}{\sqrt{R^2+H^2-2RH\cos\theta}}\right)\right]}{\tan\gamma}\right\}\right]}^{\pi/2+\sin^{-1}(ctg\,\theta_s\,ctg\,\theta)} \frac{A\cdot B\cdot C\,(G+F)}{E^2}\,d\theta\,d\phi\right] \qquad (73)$$

where θ_4 is determined again by equation (68).

For $\phi_4 > \pi$ two conditions are again considered.

If $\pi/2 - \theta_s < \theta_1$ equation (61) becomes the same as (70) except the last term is eliminated and the upper limit, θ_3 for the fourth term is replaced by θ_0.

If $\pi/2 - \theta_s > \theta_1$ equation (61) becomes the same as (72) except the last term is eliminated and the upper limit, θ_3, for the fourth term is replaced by θ_0.

For the case where the plane of the flat plate intersects the circle defined by $\theta = \theta_0$ in two points (ϕ_4, θ_0) and (ϕ_3, θ_0) for $\pi/2 - \theta_3 < \theta_1$ equation (61) becomes the same as equation (70) with the last term eliminated and the upper limits of the third and fourth terms replaced by θ_0. For $\pi/2 - \theta_3 > \theta_1$ equation (61) becomes the same as equation (72) with the last term eliminated and the upper limits of the third and fourth terms replaced by θ_0.

For $\gamma > \pi/2$ a similar step procedure in the integration of equation (61) must be used and follows the same method as set forth for $\gamma < \pi/2$ This will not be done here.

Some difficulty is encountered in determining when the plane of the flat plate cuts the sunlit region in the vicinity of the terminator. For a given ϕ_c and h to determine whether intersection of the plane and terminator occurs, the γ_2 for the plane with $\phi_c = 0$ to be tangent to the terminator was calculated

$$\gamma_2 = \cos^{-1}\left(\frac{R \sin \theta_2}{\sqrt{R^2 + H^2 - 2RH\cos\theta_2}}\right) \tag{74}$$

where $\theta_2 = \pi/2 - \theta_3$.
The maximum possible γ_0 without intersection with the sunlit area was then calculated.

$$\gamma_0 = \theta_0 \tag{75}$$

Corresponding to this point is a ϕ_{c0} that is calculated from

$$\phi_{c0} = \pi/2 - \sin^{-1}(\operatorname{ctg}\theta_3 \operatorname{ctg}\theta_0) \tag{76}$$

For a given ϕ_c the limiting γ_{lim} for intersection of the plane of the flat plate with the terminator was calculated from

$$\gamma_{lim} = \gamma_2 - \left(\frac{\gamma_2 - \gamma_0}{\phi_{c0}}\right)\phi_c$$

This is not an exact determination of the γ for tangency of the plane of the plate with the terminator circle however, the error introduced is small.

The heat flux integrals are being integrated numerically on an IBM 7090 computer. The results will be displayed in Supplement A as the geometric factor (q/PSa) as a function of altitude with the three angles, θ_s, γ and ϕ_c as parameters. A number of sheets will be required to fully display the data. Each sheet will be for a constant γ and ϕ_c.

The albedo data for a flat plate is also useful in determining albedo to an irregular surface. The irregular surface may be approximated by a series of flat plates and the albedo input is obtained by summing the individual values for each of the flat plates.

As for the other shapes considered the flat plate geometric factors may be applied to other planets using the correction factors of Table 1.

IV. Use of Natural Environment Data

As can be seen from the foregoing sections, the curves presented in Supplement A or the data tabulated in Supplement B give a complete mapping of space thermal radiation environment throughout the solar system. The data can be used directly to give the total external heat load, comprised of direct solar radiation, planetary albedo and thermal radiation, to a vehicle of a spherical, hemispherical, cylindrical, or flat surface shape located any where in space. In addition, any other shape can be evaluated by combining these shapes and/or building up a composite of flat surfaces to closely approximate the desired vehicle geometry.

It may be noted, that for distances from the planets greater than three diameters, the albedo and thermal radiation loads drop to about one percent or less, of their values close to the surface. Consequently, beyond these altitudes, these factors can for practical purposes generally be neglected. This fact, coupled with the increasing influence of planetary shadowing of solar radiation at low altitudes, makes the thermal analysis of close satellites more complex, by far, than for the case of interplanetary space.

The curves given in Supplement A are intended for use when manual computation is involved and to provide a pictoral comparison of the effects of changes in the variables controlling the heat loads. The tabulations given in Supplement B are intended for use as computer input data for automatic digital computers. It is expected that a trajectory program will be used to determine vehicle position and orientation in space as a function of time, and the incident radiation can then be automatically computed using the table look-up data and the vehicle geometry.

B. Induced Thermal Environment

For purposes of this report, the induced thermal environment consists of the thermal conditions imposed upon the vehicle due to the operation of the vehicle, its crew and equipment. It includes the heat loads generated by communication systems, vehicle guidance, attitude control and propulsion equipment, personnel and ecological systems, and whatever additional equipment and instrumentation are required for performance of the required military or scientific task.

In the case of heavily instrumented vehicles, this induced environment can become a most important factor in the thermal analysis of the vehicle. It may, in fact become a prime factor in determining the vehicle size, configuration and surface condition, as the heat must be dissipated if safe operating temperatures are to prevail. Consequently, in establishing a basis for the study of environmental control techniques, an investigation into the induced heat loads which may be expected in future space craft is fully warranted. Unfortunately, however, due to the uncertainty of future space vehicle demands and the continuously and rapidly changing state of the art, such an investigation must, at best, be only very generalized in nature. The study given in this report describes the major sources contributing to the vehicle induced heat load as they appear currently, with a discussion of the thermal contribution which they may be expected to make in the future.

Three basic types of communication systems are considered necessary. Coded transmission will require the smallest power supply. This power will be increased approximately one hundred times for voice transmission and about one hundred thousand times for television transmission. Each will have a power supply requirement varying as the square of the distance along which the signal is transmitted. (Based on this, it may be generalized that the heat radiating sections of a vehicle should have linear dimensions roughly proportional to the distance of transmission). It is clear then, that transmission system power supplies may well vary from one to millions of watts with a corresponding magnitude of effect upon the heat dissipation requirements.

Currently available radio guidance systems are capable of placing a package on the moon with an accuracy of the order of 100 miles. However, applying these systems to Venus or Mars shots, misses by several thousands of miles could be expected. Consequently, mid-course and terminal guidance systems are required. The complexity of these and complementary systems, needed to provide adequate vehicle spatial attiude, to actuate

sensors, computers, programmers, and associated equipment, will require electrical power far greater than the average current estimates of 20 watts for unmanned satellites and 50 watts for elemental manned vehicles.

Power supplies which may be required for the payload and/or instrumentation equipment to be used on military and scientific exploration vehicles cannot, at present [illegible]erly defined, due to the uncertainty concerning the types of eq[illegible]d required accuracies. About the best that can be said is t[illegible]the most part it appears that they will be designed for intermittent operation, implying that their average heat loads may be expected to be relatively low.

For manned vehicles, in space, the cabin must provide all the physiological necessities that humans find on the ground. Vital requirements of oxygen, water and food, and a safe elimination or neutralization system for disposing of metabolic products will demand electrical power which will be largely a function of the over-all duration under space conditions. The operational ecological system includes all the necessary units for maintaining safe pressurization in the cabin as well as continual control over temperature, humidity, dust, odors, microorganisms, illumination, fire hazards and other potential dangers. Missions up to about one week in space could be accomplished efficiently using storable products for man's sustenance, if only two or three men are concerned. For longer periods, up to about one month, a system of at least partial regeneration should be used. This will increase the over-all power requirement. Trips of more than ten weeks in the space must have a completely regenerative system, making a very significant increase in required power. Some authors give approximate values of 10, 100, and 1000 watts per man as estimates of power required for the three mentioned ecological system approaches.

These estimates, along with many others in this section of the report are based upon what is considered to be the best currently available information, but even so must be taken to be only approximations, as no complete designs exist for most of the future missions. Many concepts are still vague, and the efficiency of most of the systems to be used is uncertain and will undoubtedly be improved many times before their utilization. As an example, estimates of the future state of the art in communications provide values of slightly over 300 watts for television picture transmissions from Mars, as compared with the hundreds of millions as should be required today for minimum picture quality.

Humans living in the space capsule will provide additional heat loads depending upon their activity during flight. A good, all day, average estimate appears to be 500 Btu/hour-man. (Ref. 6). This is based in part on data in Table 2, which was taken from Ref. 6.

As has been pointed out, the heat dissipation by the vehicle components are not lineal functions of specific growing parameters of future missions. Some of them depending upon distance to the earth, others on the over-all duration of flight. And, of course, the number of crew members decisively effects the vehicle internal heat load. Consequently, it is clear that a precise parametric study of induced thermal environment similar to that generated for the natural thermal environment is not possible. There is included however, in Table 3, a graphic summary, or analysis, of the expected ranges of internal heat loads as a function of the type of mission. This graph is based on a general compilation of estimates made by a number of authors, primarily those in References 7, 8, and 9. The separate regions in this graph show the characteristic steps which may be expected in the space program. It is felt that this background information will provide a basis for the estimation and evaluation of environmental control systems which must be considered in the design of future space vehicles.

REFERENCES

1. Environmental Control Study of Space Vehicles (Part 1) Rodolfo M Garcia Varela and John C. Ballinger - ERR-AN-004, Convair Astronautics, Aerophysics, March 9, 1960.

2. Report of Trip to WADD, Dayton Ohio, Lewis Research Center, Cleveland, Ohio, Goddard Space Flight Center and Naval Research Laboratory in Washington D.C., and the University of Wisconsin in Madison to attend discussions on Space environmental control. Rodolfo M Garcia Varela A-TR-189, Convair Astronautics, Aerophysics February 16, 1960.

3. The Solar Constant, Francis S. Johnson, Journal of Meteorology Vol. II, No. 6, December 1954, pp 431 to 439.

4. Solar Spectral Irradiance, L. Dunkelman & R. Scolnik, Journal of the Optical Society of America, Vol. 49, No. 4, April 1959, pg. 356

5. The Observer's Handbook 1958. The Royal Astronomical Society of Canada.

6. Sealed cabins, problems of respiration and decompression. E. R. Konecci (1958), Douglas Aircraft Engineering. Paper No. 672.

7. Space Vehicles Power Systems, Eugene B. Zwick and Robert L. Zimmerman. Sunstrand Turbo Division, Pacoima, Calif. - ARS Journal, August 1959.

8. Power Supplies for Orbital and Space Vehicles, John H. Huth - Advances in Space Science, Vol. 1 Academic Press.

9. Environmental problems associated with the design and operation of space vehicle power system - Robert L. Sohn and Howard W. Wheater, Space Technology Laboratories, Inc. 1960 Proceedings of the Institute of Environmental Sciences.

TABLE I

Planet	Distance to the Sun (Astronomical Units)	Mean Radius (Nautical Miles) (R)	Solar Heat Flux (Btu/hr ft²) (S)	Albedo (a)	Planetary Thermal Radiation (Btu/hr ft²) (I_t)	Altitude Correction Factor *	Umbra Cone Apex Altitude (N.Miles)	Umbra Cone Angle (Degrees)
Mercury	0.387	1,308	2953.9	0.07	686.79	2.639	109,200	1.37
Venus	0.723	3,307	846.3	0.76	50.78	0.043	518,700	0.73
Earth	1.000	3,441	442.4	0.40	66.36	1.000	748,800	0.53
Mars	1.524	1,799	190.5	0.15	40.48	1.916	592,400	0.35
Jupiter	5.203	37,758	16.4	0.51	1.98	.091	48,974,000	0.09
Saturn	9.539	31,067	4.9	0.50	0.61	.111	69,477,000	0.05
Uranus	19.18	18,818	1.2	0.66	0.10	.269	54,739,000	0.03
Neptune	30.06	11,645	0.5	0.62	0.05	.296	77,686,000	0.02
Pluto	39.52	1,564	0.3	0.16	0.06	2.203	13,347,000	0.01
Moon	1.000	938	442.4	0.07	102.86	3.676	202,200	0.53

* To use the albedo and thermal radiation curves and tabular data for a planet other than the earth, an equivalent earth altitude for the planet must be found. This may be done by multiplying the planetary altitude under consideration by the altitude correction factor given in the above table. The abscissa of the curves should then be entered with this corrected altitude.

Example: Thermal radiation to a sphere 200n.mi. above the surface of Mars.

$200 \times 1.916 = 383.2$ n.mi.

From Fig. 3, $q/\pi r^2 I_t = 1.12$

Using I_t for Mars gives $q/\pi r^2 = 45.3$ Btu/hr-ft^2

Table 2

Estimated Daily Energy Expenditure for an Average Man in a Sealed Cabin

Condition	Duration	Energy Expenditure	
	(hr)	(kcal/hr)	(kcal/day)
Sleep	8	65	520
Light work	8	150	1200
Rest sitting	5	100	500
Rest laying	1	80	80
Light exercise	1	200	200
Heavy exercise or work	1	500	500
Total	24		3000

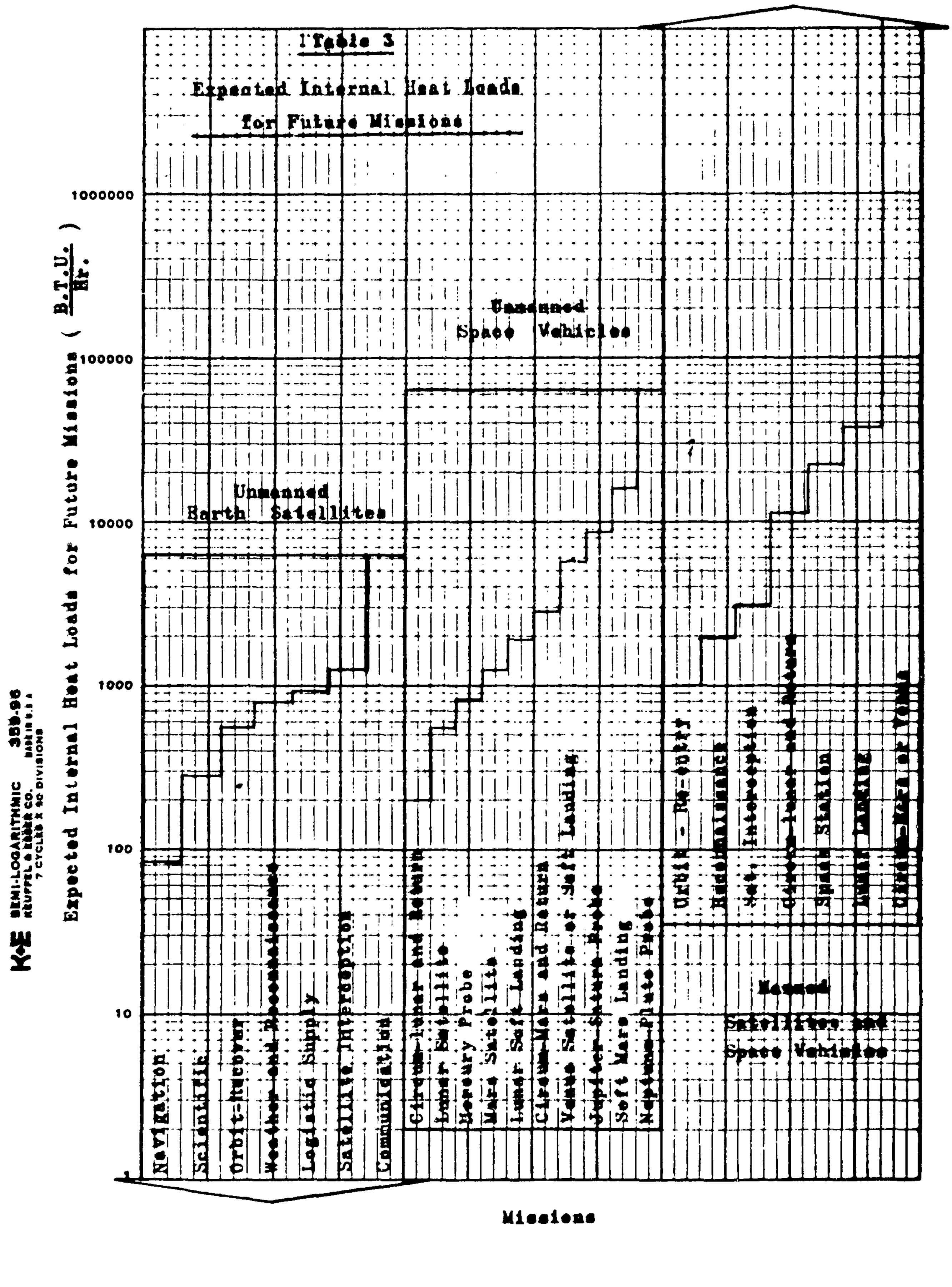
Table 3
Expected Internal Heat Loads for Future Missions
Unmanned Earth Satellites
Unmanned Space Vehicles
Manned Satellites and Space Vehicles
Expected Internal Heat Loads for Future Missions (B.T.U./Hr.)
1000000
100000
10000
1000
100
10
1
Navigation
Scientific
Orbit-Recovery
Logistic Supply
Satellite Interception
Communication
Circum-lunar and Return
Lunar Satellite
Mercury Probe
Mars Satellite
Lunar Soft Landing
Circum-Mars and Return
Venus Satellite or Soft Landing
Soft Mars Landing
Orbit - Re-entry
Sat. Interception
Space Station
Missions
K+E SEMI-LOGARITHMIC 359-90
KEUFFEL & ESSER CO.
7 CYCLES X 90 DIVISIONS

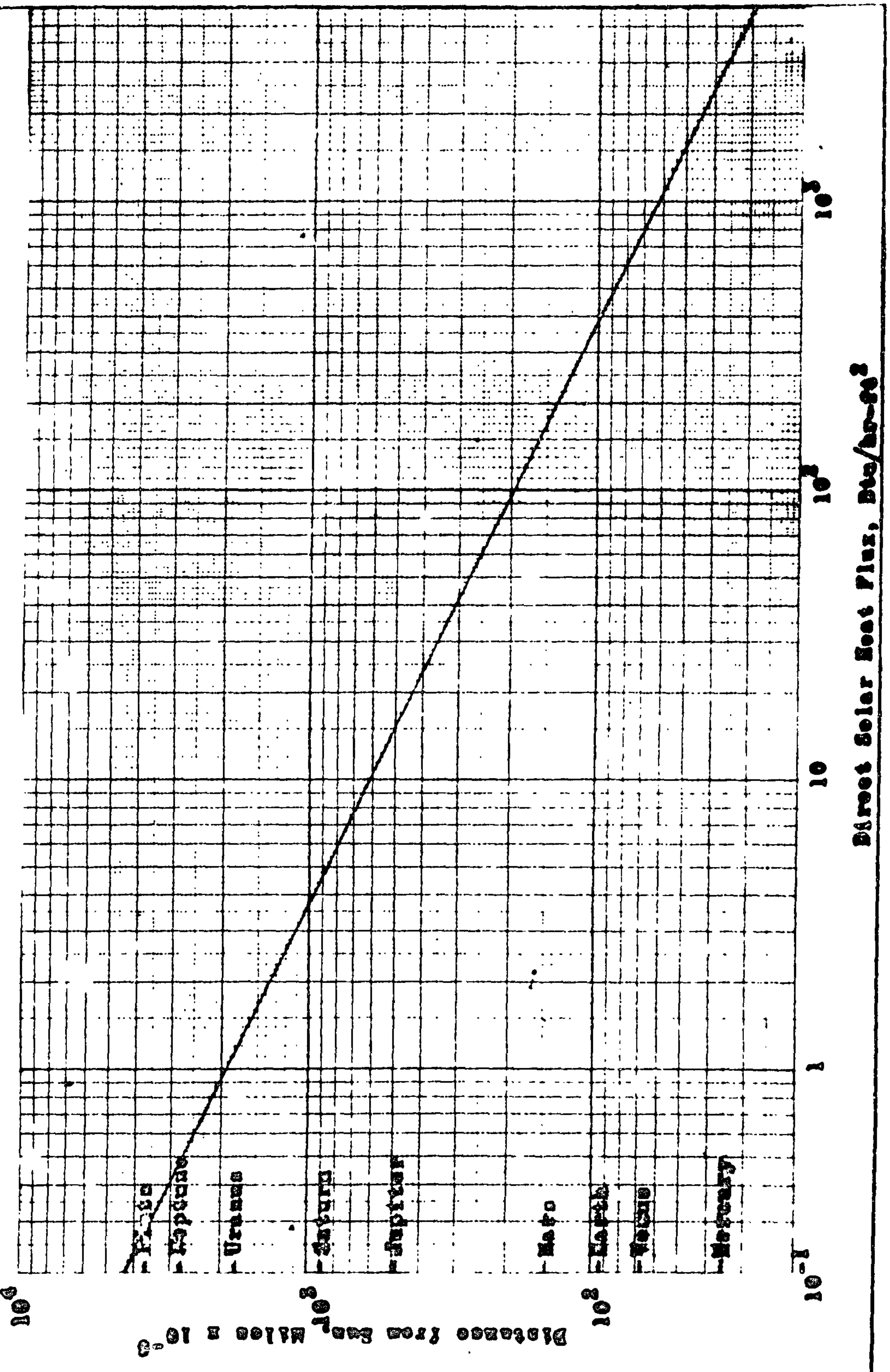

Fig. 1 - Variation of the Solar Heat Flux With the Distance to the Sun

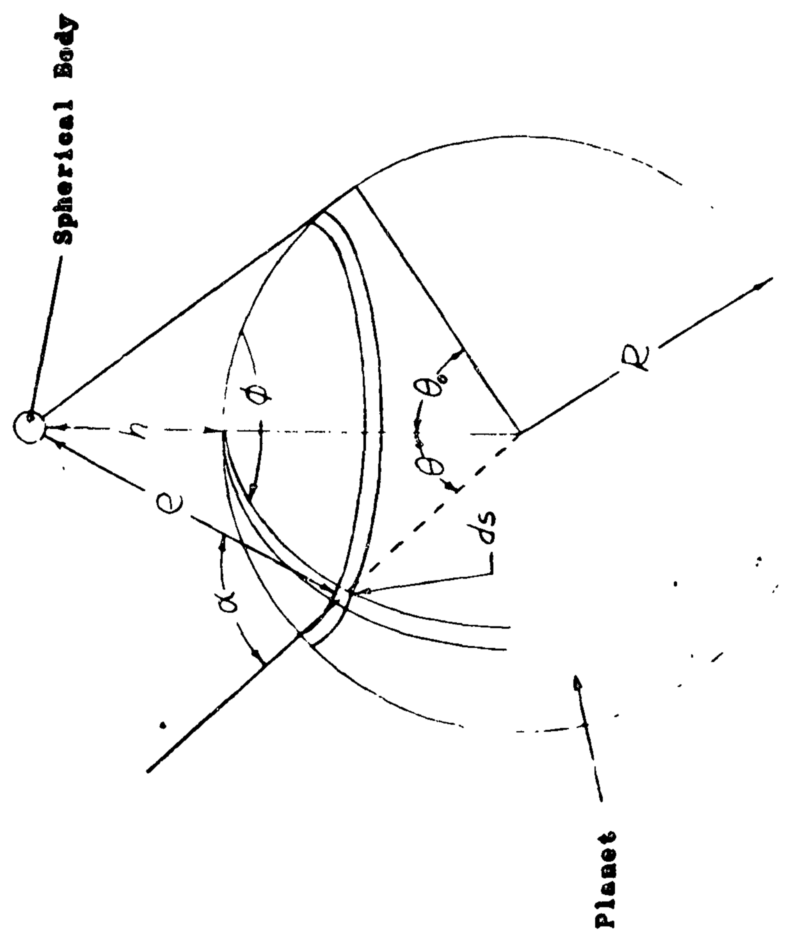

Fig. 2 - Geometry of Planetary Thermal Radiation to a Sphere

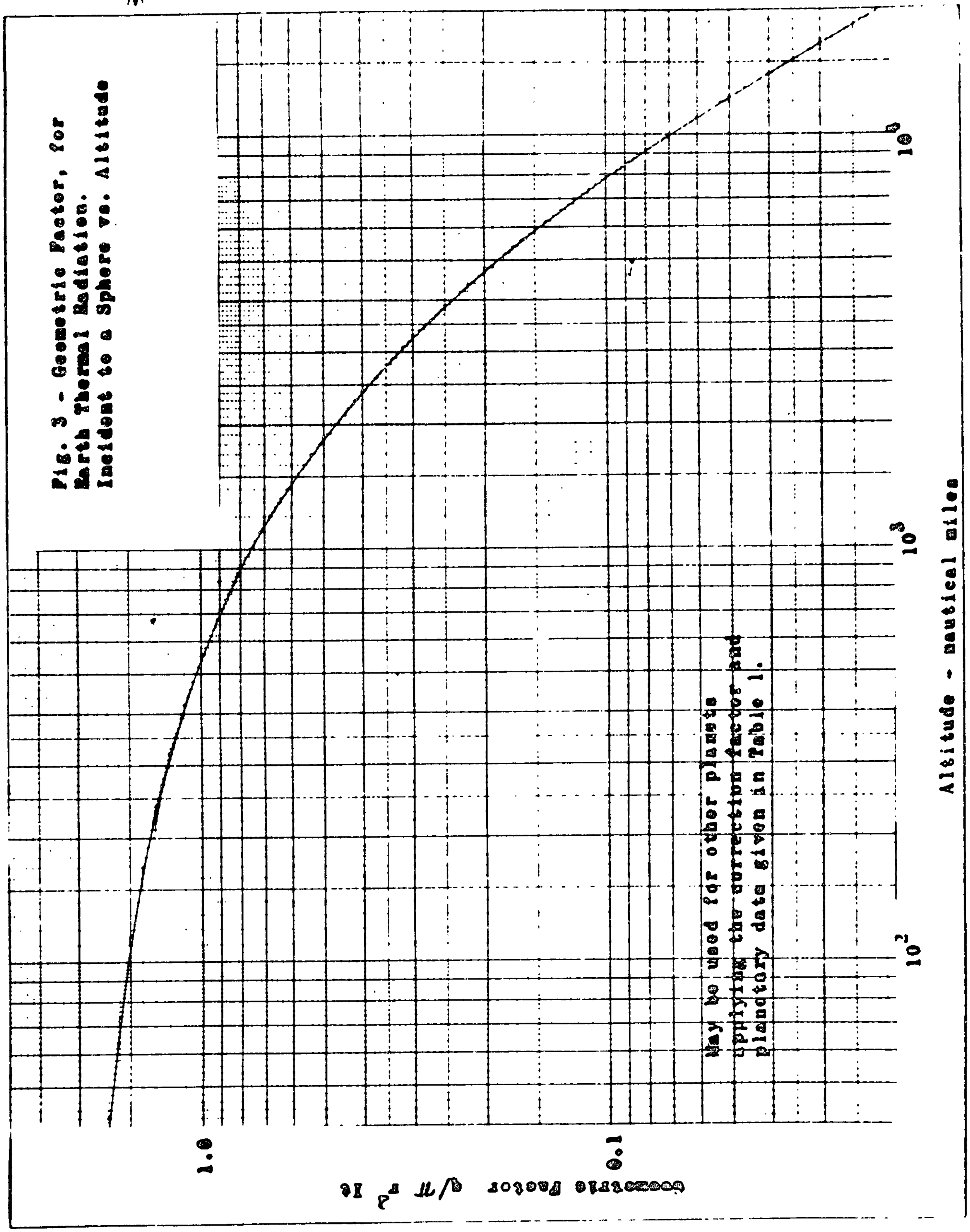

Fig. 3 - Geometric Factor, for Earth Thermal Radiation. Incident to a Sphere vs. Altitude

Fig. 4 - Geometry of Thermal Radiation to a Cylinder

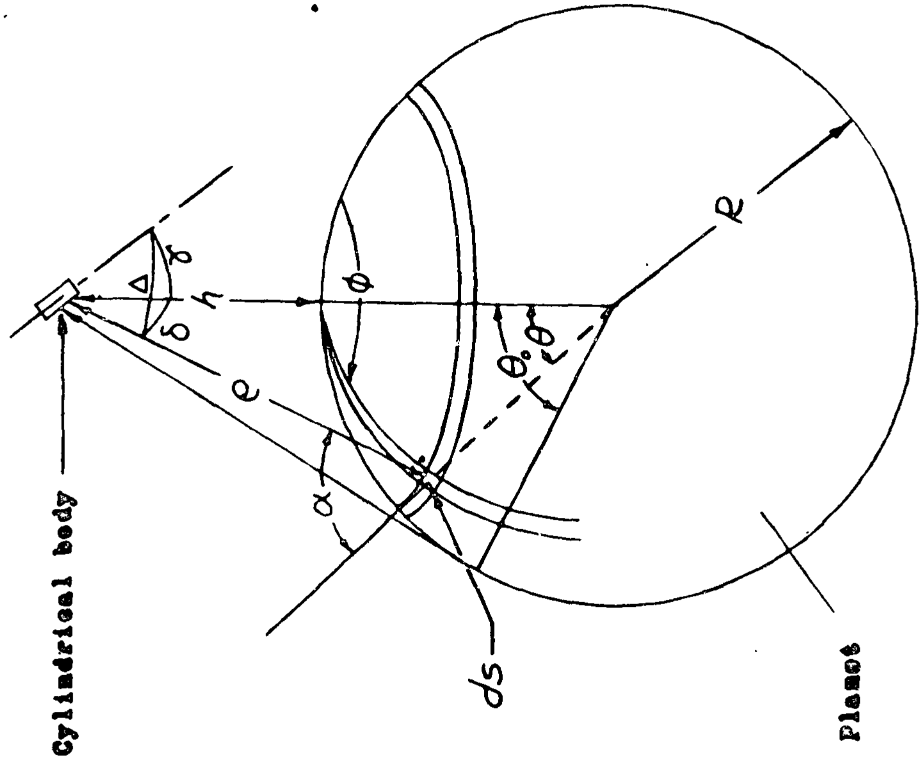

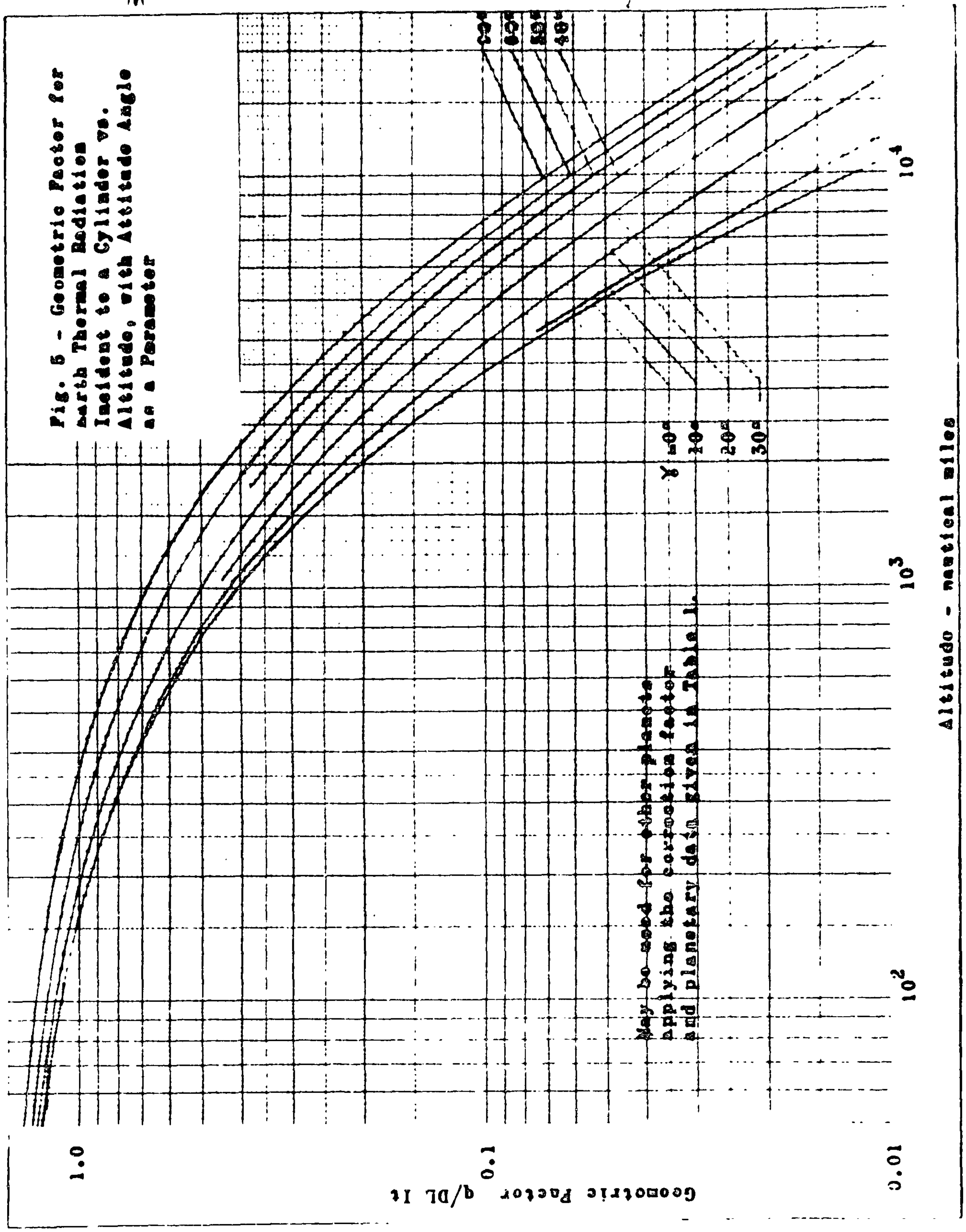

Fig. 5 - Geometric Factor for Earth Thermal Radiation Incident to a Cylinder vs. Altitude, with Attitude Angle as a Parameter

Fig. 6 - Geometry of Thermal Radiation to a Hemisphere

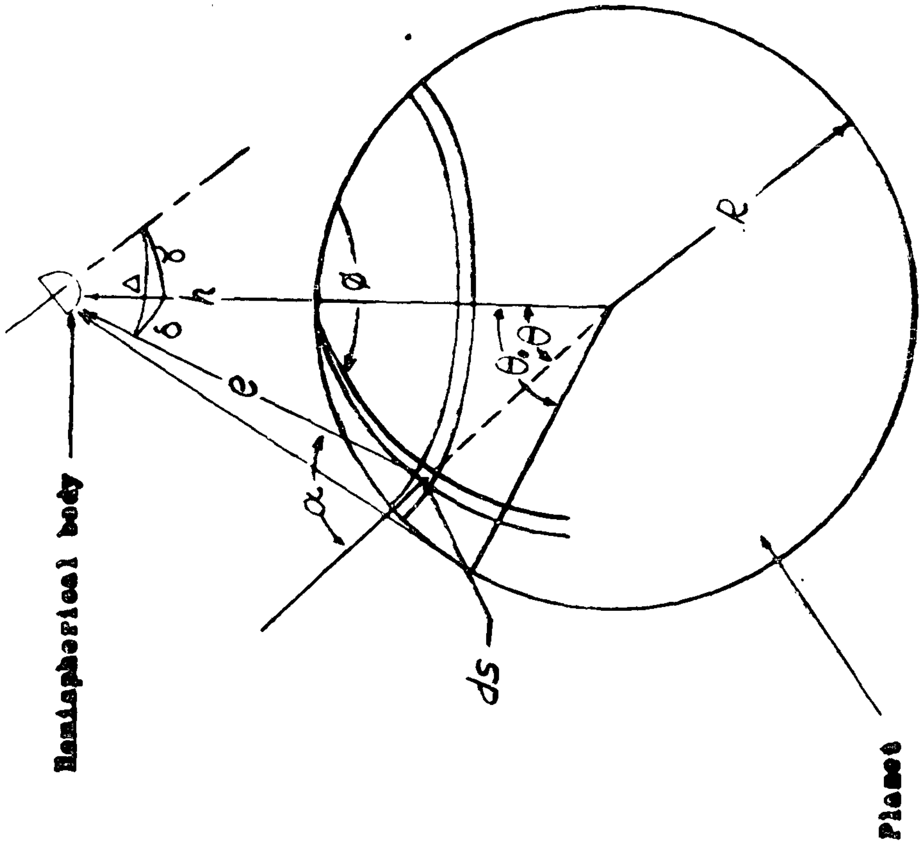

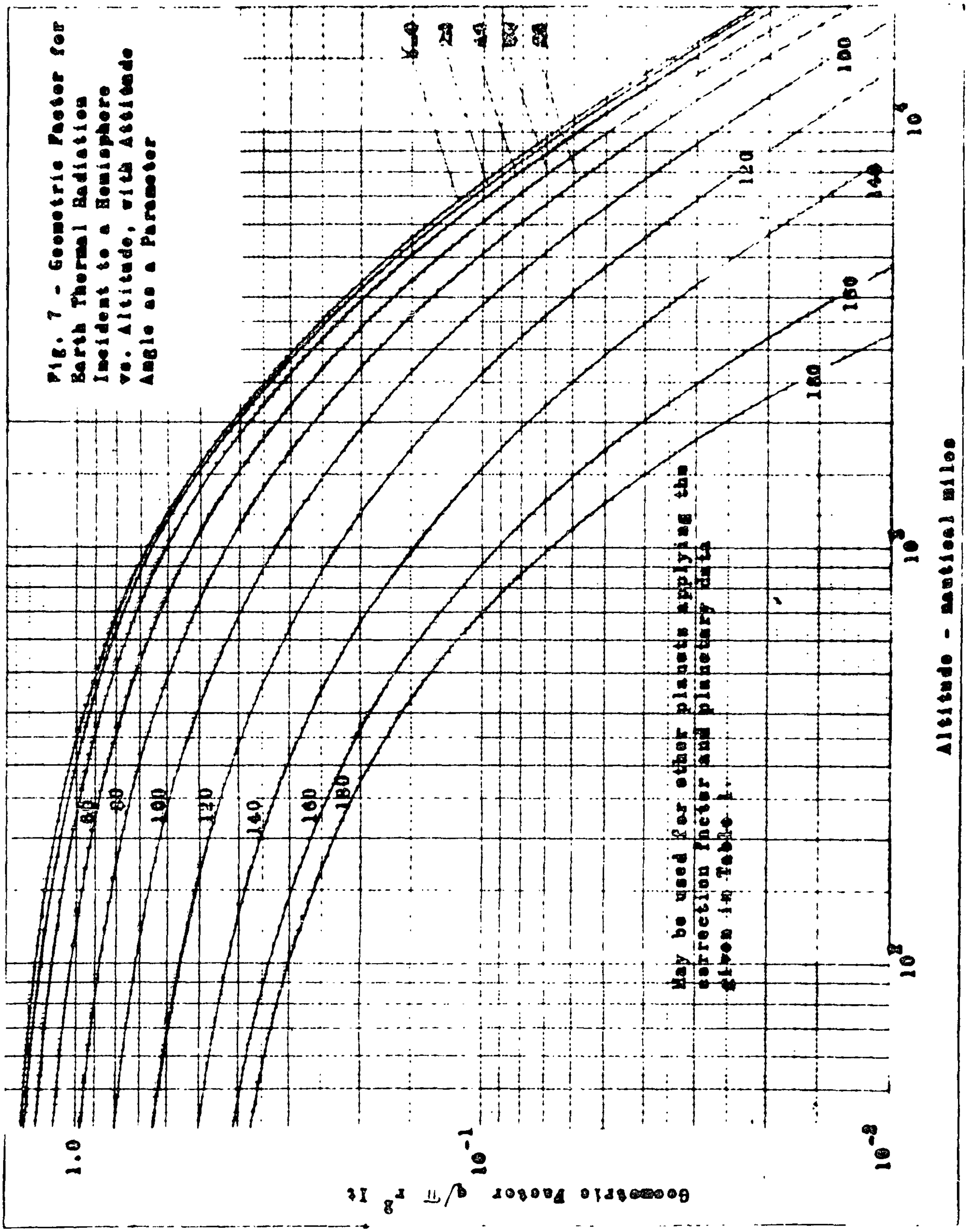

Fig. 7 - Geometric Factor for Earth Thermal Radiation Incident to a Hemisphere vs. Altitude, with Attitude Angle as a Parameter

Fig. 8 - Geometry of Thermal Radiation to a Flat Plate

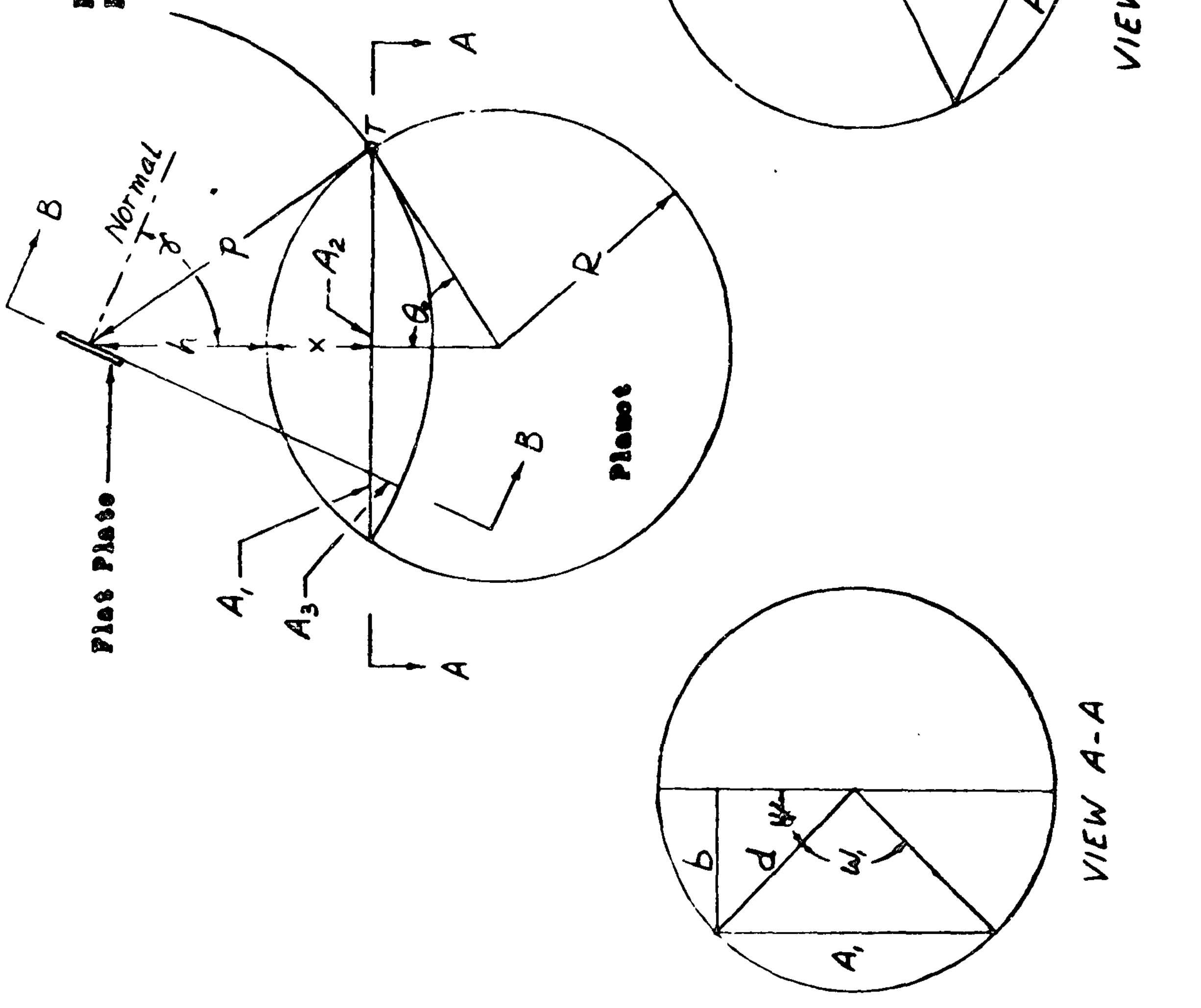

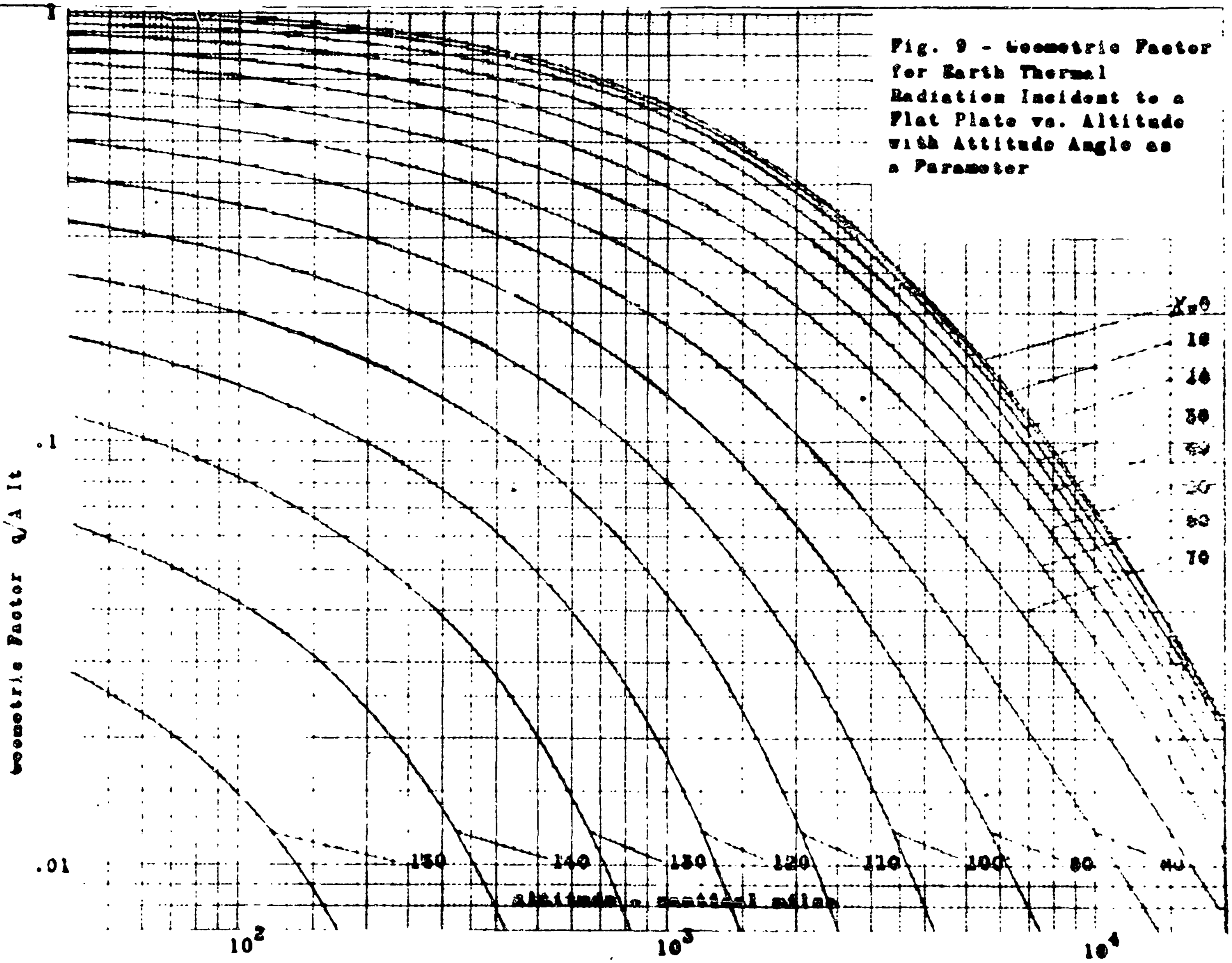

Fig. 9 - Geometric Factor for Earth Thermal Radiation Incident to a Flat Plate vs. Altitude with Attitude Angle as a Parameter

May be used for other planets applying the correction factor and planetary data given in Table 1

Fig. 10 - Geometry of Planetary Albedo to a Sphere

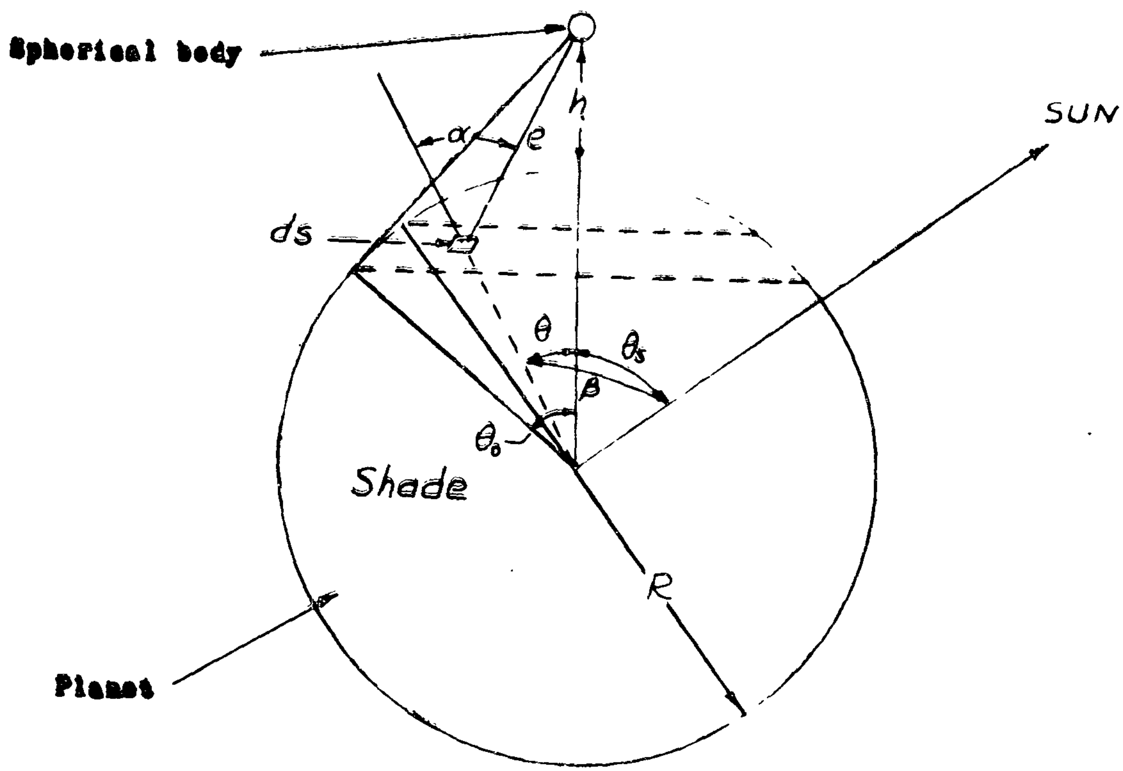

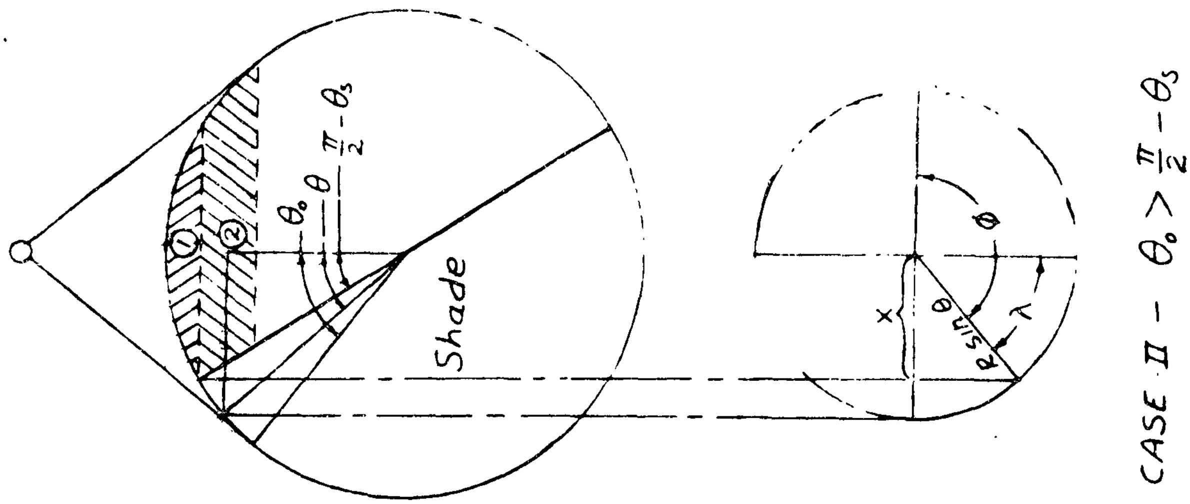

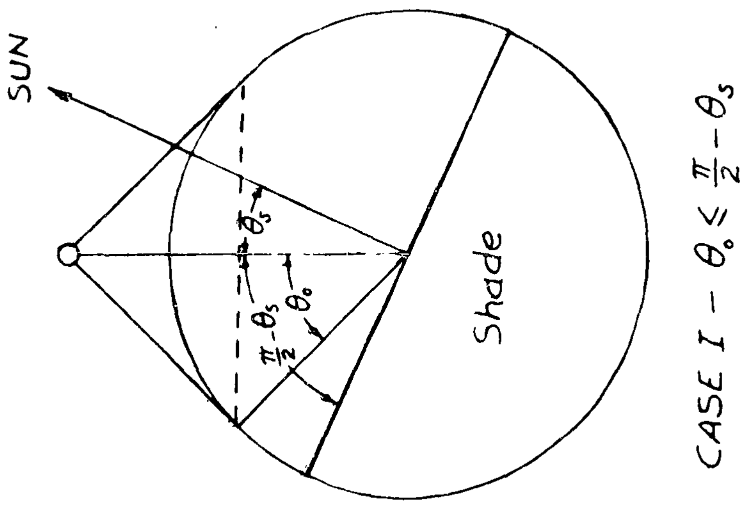

Fig. 11 - Cases for the Limits of Integration in Albedo to a Sphere

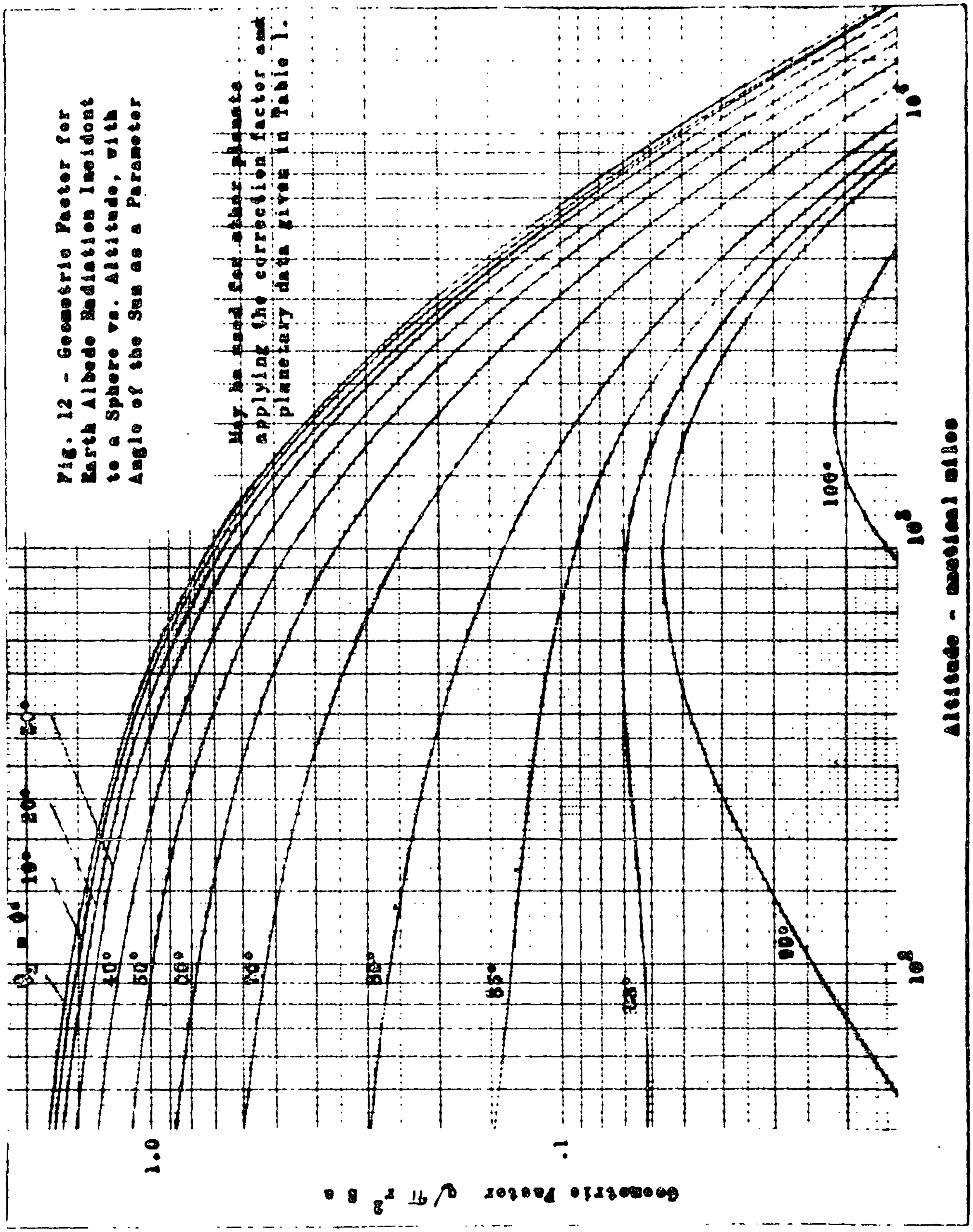

Fig. 12 - Geometric Factor for Earth Albedo Radiation Incident to a Sphere vs. Altitude, with Angle of the Sun as a Parameter

May be used for other planets applying the correction factor and planetary data given in Table 1.

Figure 13. Geometry of Planetary Albedo to a Cylinder

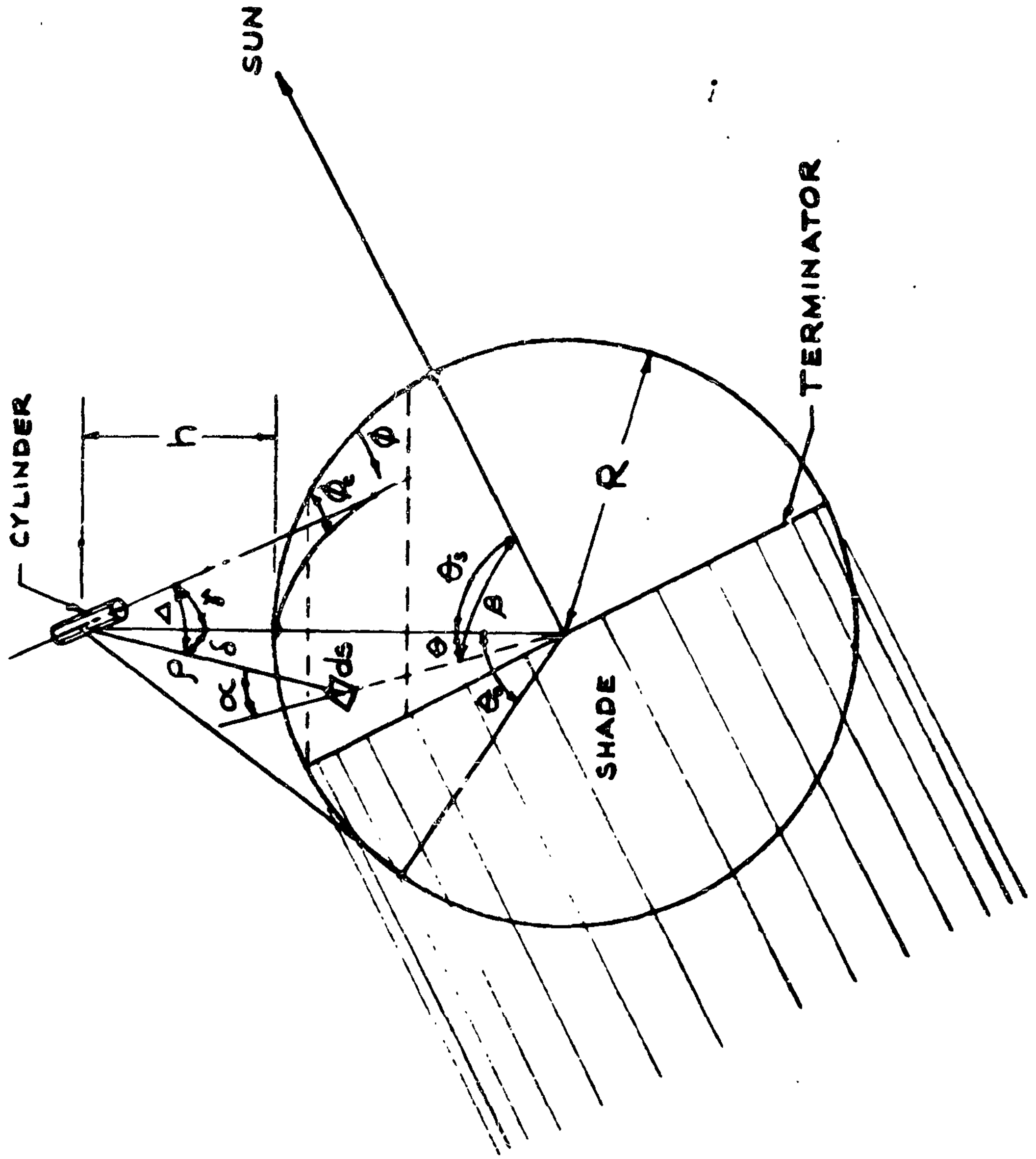

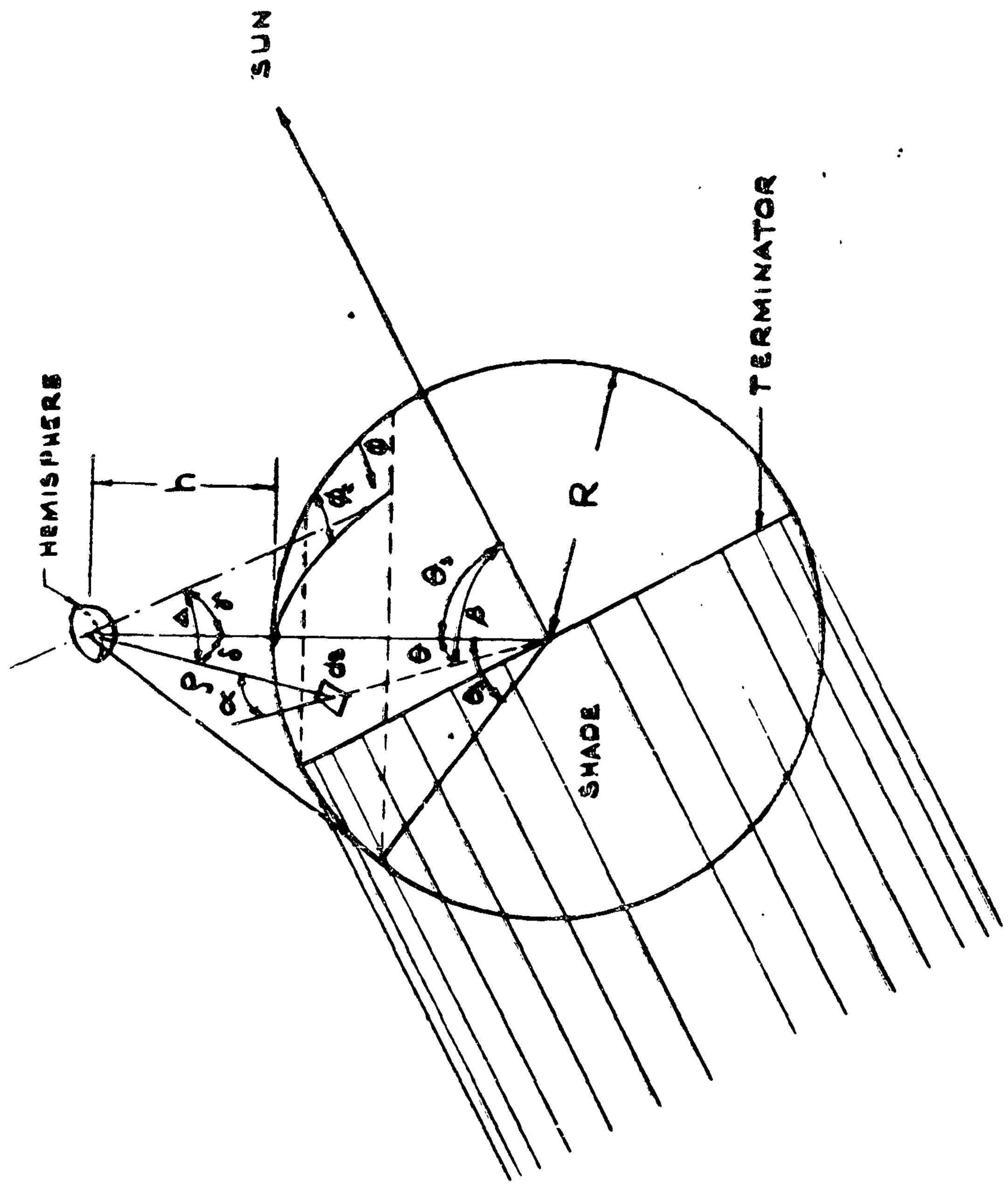

Figure 14. Geometry of Planetary Albedo to a Hemisphere

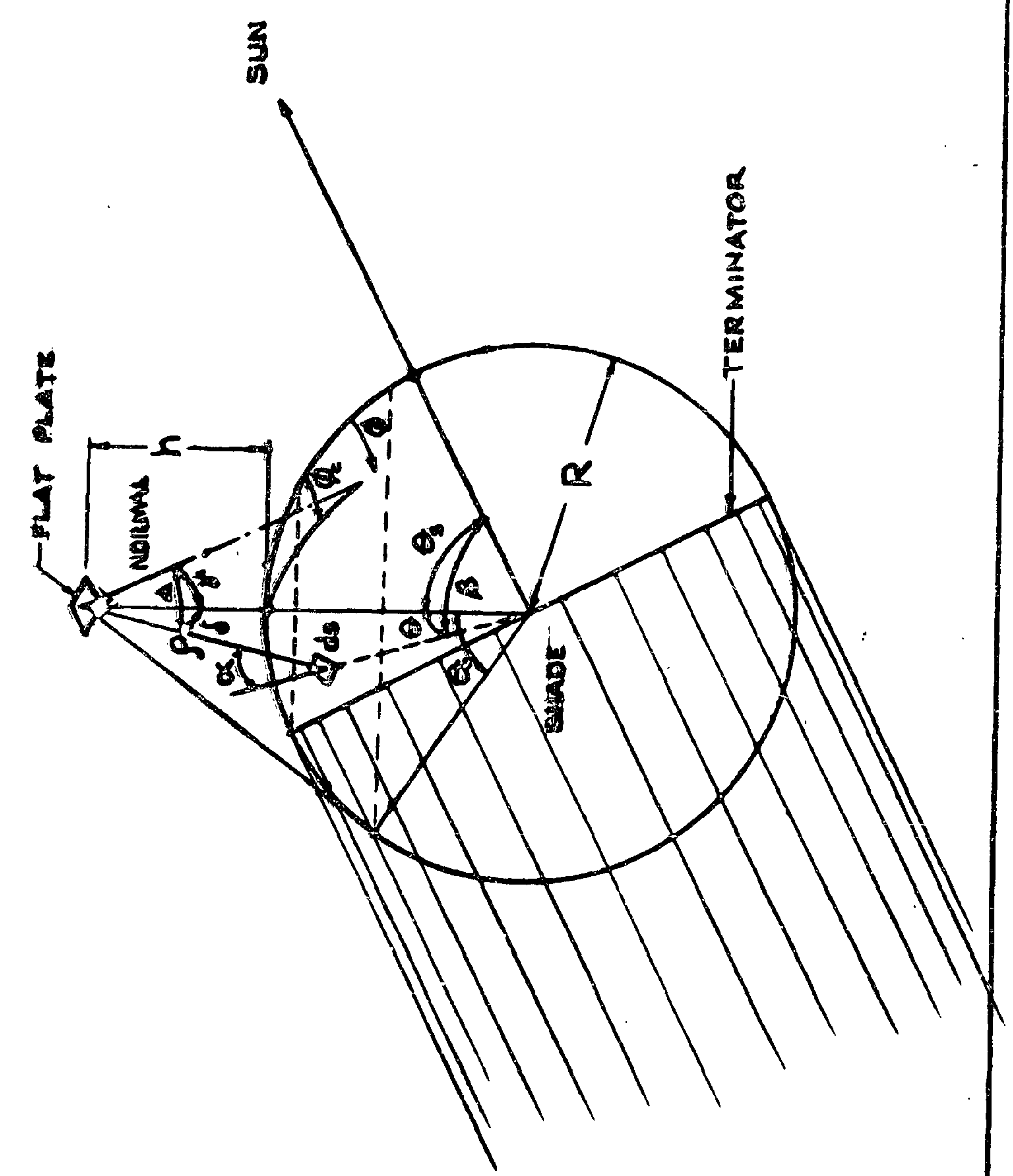

Figure 15. Geometry of Planetary Albedo to a Flat Plate

DISTRIBUTION

	Mail Zone	No. of Copies
General Office		
R. C. Sebold	1-710	1
I. M. Nestingen	1-713	1
R. J. Lutz	1-711	1
San Diego Division		
C. W. Frick	6-103	3
F. Haas	6-103A	1
R. F. H[illegible]	6-103A	1
E. Oertel/W. Boyce	7-01	1
Division Library	6-157	1
J. M. Bowyer, Jr.	6-105	1
E. J. Steeger	63-20	1
C. Jackson	6-173	1
Fort Worth Division		
E. L. Secrest	6-2	3
Division Library	571	1
L. H. Schreiber	6-2	2
R. N. Oliver	6-2	2
J. Fernandez	6-2	2
Pomona Division		
G. E. Burkheimer	6-18	3
J. M. Guthrie	6-73	1
Division Library		1
Astronautics Division		
H. F. Dunholter	590-00	1
F. J. Dore	593-00	1
W. F. Radcliffe	595-00	1
Division Library	521-50	2
C. C. Love	593-1	1
J. Guill	593-1	1
H. B. Steele	593-1	1
N. O'Rourke	593-1	1
F. A. Ford	593-1	1
W. B. Mitchell	595-1	1
J. C. Ballinger	595-1	10